NPR

Applications of Isothermal Titration Calorimetry as a Powerful Tool to Study Natural Product Interactions

Journal Name

ARTICLE

Application of Isothermal Titration Calorimetry as a Tool to Study Natural Product Interactions

O. Callies and A. H. Daranas[*]

Covering: up to February 2015

Over the past twenty-five years, isothermal titration calorimetry (ITC) has become a potent tool for the study a great variety of molecular interactions. This technique is able to provide a complete thermodynamic profile of an interaction process in a single experiment, with a series of advantages in comparison to other comparable techniques, such as less amount of sample or no need of chemical modification or labelling. It is thus not surprising that ITC has been applied to study the manifold types of interactions of natural products to get new insights into the molecular key factors implied in the complexation process of this type of compounds. This review provides an overview over the applications of ITC as a potent tool to investigate interactions of natural products with proteins, nucleic acids, oligosaccharides, and other types of receptors. The examples have been selected depending on the impact that this technique had during the investigation and revision of the interactions involved in the bioactivity of a compound, lead optimization or technical applications.

1 Introduction
2 Applications of Isothermal Titration Calorimetry in Protein–Natural Product Interactions
2.1 Protein–polyphenol interactions
2.2 Interaction of Proteins with Amines, Amides and Peptides
2.3 Protein–Alkaloid Interactions
2.4 Protein–Terpene Interactions
2.5 Interactions of Proteins with other Natural Products
3 Nucleotide–Natural Product Interactions
4 Cyclodextrin–Natural Product Interactions
5 Other Natural Product Interactions

1 Introduction

Molecular association is a fundamental phenomenon in almost all aspects of biological, chemical, and physical processes. They all have in common energetic changes and result in a release or consumption of heat from the environment. These energetic variations can be measured and provide valuable information on the specific characteristics of the interaction. Although different methods have been developed to analyse molecular association events, such as surface plasmon resonance (SPR) or nuclear magnetic resonance (NMR) spectroscopy[1], isothermal titration calorimetry (ITC) is unique. Its advantage is that it is able to provide a complete thermodynamic[2] and even kinetic[3] profiling in a single

experiment, with a small amount of sample and without the need of any chemical modification, giving direct measurement of the binding constant, the stoichiometry, and the heat of reaction, and indirect access to other thermodynamic parameters like entropic binding contribution or Gibbs free energy.[4] ITC is robust and can be used to determine binding affinities in the range from 100 μM to 1 nM,[5] sometimes with less than 500 μg of receptor to conduct a complete calorimetric profile with accuracies better than 0.4 kJ mol^{-1}.[6] Alternative experimental designs that may include the use of competitive ligands have been proposed to study very high or low affinity interactions.[7–9]

Over the past twenty years, a detailed description of theory and practice of ITC has been the topic of various reports.[10–17] The general procedure to perform a typical ITC experiment consists in a titration of ligand aliquots into a receptor solution, and the heat that is released (exothermic reaction) or taken up (endothermic process) is registered in relation to a reference cell.[2] In some cases, such as to resolve the cooperative thermodynamics of macromolecules with multiple binding sites, reverse ITC experiments, where titrant and receptor locations are reversed, can deliver better results.[18] Furthermore, if the aim of an experiment is only the determination of the enthalpy change of a binding process, this can be obtained by a single injection or a small number of additions of a ligand.[4]
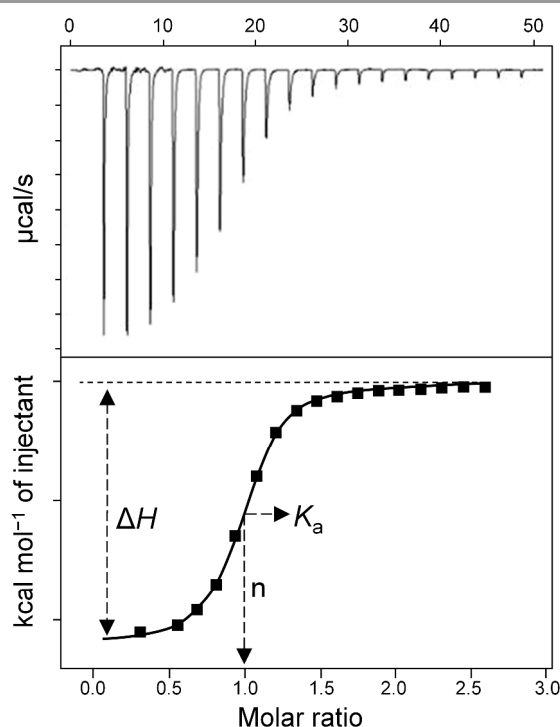
Fig. 1 Typical titration profile of an ITC experiment. The upper panel shows the recorded power as a function of time. Each peak represents the heat produced upon a ligand aliquot injection into the receptor solution within the calorimetric cell. Heats are determined by peak integration. The resulting titration curve (lower panel) shows the heats of binding as a function of molar ratio. Non-linear least-squares analysis allows determination of the parameters ΔH, n, and K_a.

The experimental output is a plot of the recorded power that is necessary to maintain constant temperature as a function of time, where each peak represents the thermal effect caused by each injection (Fig. 1).[11] The area under each peak represents heat energy changes upon ligand injection. During the titration process, the binding site becomes more saturated, a situation which is reflected in a decrease of the observed heats.[4] If the titration reaches adequate saturation the observed peaks with constant values will be representative of the corresponding dilution heats. The subtraction of an average value of these final injections is probably the best option to remove dilution effects from binding data.

At this point it is important to consider that, in order to obtain any thermodynamic parameter, the raw data has to be fitted using a model and that the chosen one might not be an accurate description of the binding event. This fitting process is generally undertaken using the so-called Wiseman isotherm. Wiseman *et al.*[19] showed that a new parameter c, defined as the product of the binding affinity K_a and the receptor concentration $[R]$ in the cell (equation 1), has to be within values of 1 and 1000 for the reaction to be appropriately characterized by ITC.

$$c = nK_a \cdot [R]_t \qquad (1)$$

From a practical point of view, this statement restricts the dissociation constants that can be studied from 10^{-4} to 10^{-9} M

approximately. However, solutions to extend this limited range have been proposed either by making use of an appropriate experimental design for low affinity ligands or by competition experiments for high-affinity ligands.[8,9] Furthermore, misperceptions derived from an incorrect model selection can be avoided using structural information about the system under study, in particular about the number of binding sites, but also using the recently proposed differential binding models that rely on more general assumptions.[20]

The whole set of peaks gives the titration curve, whose amplitude is proportional to the enthalpy of the interaction (ΔH), where the corresponding stoichiometry (n) is given by the inflection point, and where the slope yields the binding affinity (K_a) or dissociation constant ($K_d = 1/K_a$) in case of sigmoidal titration curves (Fig. 1).[5] K_a describes the ratio of concentration of a complex (R–L) at equilibrium for a reversible reaction between a free receptor (R) and a ligand (L), as shown in equation (2).

$$K_a = [R{-}L]/([R][L]) \qquad (2)$$

As K_a is linked to the change in the Gibbs free energy (ΔG), according to the van't Hoff relationship (3)[13]

$$\Delta G = -RT \cdot \ln K_a \qquad (3)$$

in which R is the gas constant (8.314 J K^{-1} mol^{-1}) and T is the absolute temperature in Kelvin, the value of ΔG can be determined. To calculate the logarithm in equation (3), it is necessary to transform K_a, with units of inverse concentration, into a unitless parameter (K_a^o). This is done by normalizing concentrations to the standard state concentration $C_0 = 1$ M following equation (4).

$$K_a^o = K_a \cdot C_0 \qquad (4)$$

This normalization of thermodynamic properties into their standard states (ΔG^o, ΔH^o, ΔS^o) is valuable to compare reported values.[21] The entropic binding contribution (ΔS^o) can be calculated as numerical difference between the Gibbs free energy ΔG^o and enthalpy ΔH^o through

$$\Delta G^o = \Delta H^o - T\Delta S^o \qquad (5)$$

It is worth noting that ITC directly determines only K_a and ΔH^o, whereas ΔG^o and ΔS^o are calculated from them using equations (3) and (5). This is particularly important in error propagation: while ΔG^o shows a logarithmic dependence on K_a and, in consequence, the transmitted absolute error is rather small, any error in ΔH^o results in a correlated one of comparable magnitude in ΔS^o. As a result, artificial enthalpy/entropy compensation will emerge. This phenomenon is particularly important in the analysis of thermodynamic data, and considerable debate exists about the physicochemical mechanisms underpinning it.[22] The simplest explanation for this compensation would be that a favourable enthalpy change upon ligand binding (increasing the number of specific interactions between receptor and ligand) would be linked to a

conformational restriction of the ligand with the resultant unfavourable change in entropy. However, there is abundant literature suggesting that solvent reorganization could be responsible of this effect.[23] More complex explanations include receptor flexibility as a source of compensation.[24]

Although most sources of error in an ITC experiment are now well known, some of them are routinely overlooked. On the one hand, the most important cause of error is generally linked to an inadequate quantification of ligand concentration, and standard fitting procedures translate this error directly into the calculated K_a and ΔH^o values.[25] On the other hand, receptor concentration is treated as a variable in the fitting procedure, and the corresponding errors are translated to the stoichiometry calculation. Thus, as ITC only measures the "active" receptor concentration, protein degradation can be a possible source of error. Unfortunately, in general, reported errors merely describe those derived from the nonlinear fit procedure and omit those coming from concentration inaccuracies.

It has to be underlined, that ΔH^o values obtained by ITC represents the overall energy change of the process, including dilution and binding heats, solvation energy, and other energy variations due to conformational changes, and, thus, do not represent absolute ΔH^o values.[13] In particular, the ITC user has to keep in mind the effects of the chosen buffer, as the observed enthalpy ΔH_{obs} includes the heat of protonation reactions which is characteristic of each buffer. Thus, a titration involving a variation in protonation state can easily change from an endothermic to an exothermic reaction with the move to another buffer system. Nevertheless, the intrinsic enthalpy change ΔH_o can be obtained by performing experiments using buffers of different ionization enthalpies.[26] In addition, if ITC experiments are done at different pH values, the pK_a of the involved group can be determined.[27] Another important experimental buffer-related consideration is the necessary matching between the cell and the syringe content, because little differences in pH could generate large background heats depending on ionization enthalpies.

Another point to consider is that, according to the van't Hoff equation (3) and equation (5), temperature has an effect on the measured thermodynamic parameters through

$$\ln K_a = -\frac{\Delta H}{RT} + \frac{\Delta S}{R} \qquad (6)$$

Thus, measurement of ΔH at different temperatures enables the calculation of the binding heat capacity at constant pressure ΔC_p according to equation (7).[2]

$$\Delta C_p = \partial \Delta H / \partial T \qquad (7)$$

From this relationship it comes that a reaction with a negative heat capacity change will become increasingly enthalpic and less entropic with increasing temperature, while opposite behaviour will be observed for those with positive heat capacities. Therefore, it is clear that the experimental temperature is an important parameter to consider when discussing if a particular reaction is enthalpically or entropically driven.

Finally, the interpretation of the obtained calorimetric results can indicate the correspondent physical phenomena driving the interaction. That way, largely favourable enthalpic contributions are assigned to van der Waals interactions, hydrogen bonding, or electrostatic interactions that are counter partnered by the unfavourable enthalpy change associated with the desolvation of polar groups. Largely entropy-dominated processes are indicative for changes in the solvation of lipophilic and/or hydrophobic groups that originates from the release of water molecules from the binding pocket upon complexation. By contrast, conformational changes involving the loss of degrees of freedom are generally unfavourable in entropic terms.[22]

The aim to get a detailed understanding of the structure-function relationships of the different receptor-ligand interactions are of great interest for molecular life sciences, as the manifold interactions of small molecules are fundamental both for the biological activities of many pharmacologically important compounds and for a broad variety of different biological processes.[12] Thus, while a static crystallographic structure is clearly suggestive to explain a biomolecular interaction, the key to understanding the affinity of a ligand to its receptor lies in the thermodynamics of the association. Therefore, ITC presents a potent technique to expand the "classical" machinery of biophysical methods, such as NMR or biological assays, generally used for lead optimization purposes of natural products (NPs) in preclinical stages, and to get new and deeper insights into the mechanisms of action of these secondary metabolites to facilitate the development of new and more potent drugs for a future application in the clinic.[6]

These characteristics make ITC a technique that can be applied in a multi-disciplinary field, ranging from material science[36], quality control[11], and nanotechnology[37], to medicinal chemistry, drug design[4,6,38], or biology.[1,14,39–41] That way, the thermodynamic requirements of interactions as diverse as macromolecular complex formation, polymer interactions, micelle formation, permeation through lipids, low or high affinity interactions, investigation of biosynthetic routes, or even biological processes in living systems can be studied in detail.

One of the classic applications of ITC studies is the investigation of potential relationships between structure and thermodynamics of protein–ligand interactions and for most of which structural information is available. In contrast, this review will focus on the application of ITC in the field of natural products research, providing an overview of structural diverse natural product interactions with proteins, polynucleotides and oligosaccharides, as well as interactions with some less investigated receptors, such as lipids or inorganic compounds. The added value of this technique is outlined as it delivers insights into unknown interactions and is able to get novel insights into interactions that were thought to be fully understood. Some new ITC applications, such as the use of living cells, are also discussed.

2 Applications of Isothermal Titration Calorimetry in Protein–Natural Product Interactions

Certainly the most important type of interaction of natural products is that with proteins, as they present their counterpart in a broad range of biological activities. In this context, natural polyphenols, amines, amides, peptides, alkaloids, and terpenes are implicated in properties such as wine adstingency, but also act as antioxidants or exhibit biological activities in cancer, amyloidoises, diabetes, and hormonal imbalances. Furthermore, affinity of natural products to blood proteins is important for their distribution and can give helpful insights for further preclinical developments. Although, in general, ITC experiments can be conducted with almost all classes of proteins, issues such as aqueous solubility, potential conformational changes, and membrane localization are important considerations to design the most adequate experimental protocol and control experiments. As a result, the combination of thermodynamic data with high-resolution structural information can help to select more accurately the lead compounds for further investigation and optimization of drug–target interactions. It is thus not surprising that natural product–protein interactions are one of the classic applications of ITC studies as it can deduced by the important number of available papers in the field.

2.1 Protein–Polyphenol Interactions

Within the application of ITC in protein–natural product interactions, polyphenolic compounds, such as anthraquinones, or flavonoids, are among the most described. These type of interactions are implicated in beverages astringency[34,35], antioxidant activity, cancer prevention[36–39], drug distribution[40–43], amyloidoises[44–47], bacterial resistance[48], and diabetes.[49] Therefore, the evaluation of the thermodynamic basis of these phenomena are of interest in particular for drug development. Literature indicate that, in general, hydrophobic interactions and hydrogen bonding are responsible for protein–polyphenol interactions, whereas reports on the implication of covalent interactions are contradictory.[41,50] Thus, ITC is an attractive approach for the study of protein–polyphenol interactions to get further insights into the involved mechanisms, in particular as this technique can be applied to study insoluble complexes, as is often the case for protein–polyphenol systems.[41]

Evaluation of Polyphenols in Astringency. Flavan-3-ols (Fig. 2) are polyphenolic compounds present in fruits, cacao, and in beverages such as wine. Their well-known potential to interact with proteins is responsible, for example, for astringency. Astringency is produced from the loss of lubrication in the oral cavity as a result of precipitation of salivary proteins, which are rich in proline. Furthermore, this phenomenon is an important feature of red wine and plays a significant role in its quality. Thus, there are different studies in which astringency was investigated using ITC.

Poncet-Legrand *et al.*[34] investigated the binding of four flavan-3-ol monomers (catechin, epicatechin, epicatechin gallate, and epigallocatechin gallate, Fig. 2A–C) and an
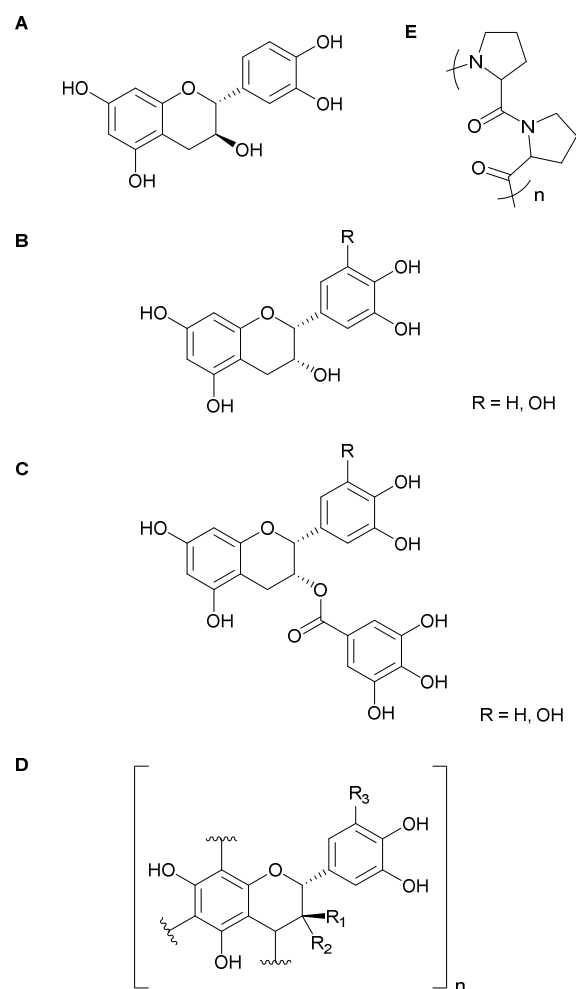
Fig. 2 Polyphenols and receptor used in the evaluation of astringency. A, catechin; **B**, epicatechin (R=H) and epigallocatechin (R=OH); **C**, epicatechin gallate (R=H) and epigallocatechin gallate (R=OH); **D**, grape seed tannins: The indicated attatchment points correspond to interflavanal linkages; R_1, R_2 and R_3 can vary corresponding to catechin structures **A–C**; **D**, poly(L-proline);

oligomeric fraction of grape seed tannins (Fig. 2D) to proline-rich human salivary proteins by means of ITC, as well as the mechanisms involved in galloyl-dependent particle formation. Experiments were carried out at pH 3.6, corresponding to the acidity of wine, and, in place of human salivary proteins, whose ITC results are difficult to interpret, they used poly(L-proline) (Fig. 2E). Analysis of ITC data showed that all interactions were exothermic with the implication of coexistent enthalpy- and entropy-driven phenomena. When comparing the heat changes of catechin (Fig. 2A) and epicatechin (Fig. 2B) with those of the galloylated monomers (Fig. 2C), no interaction was observed in the case of non-galloylated monomers. This observation was in agreement with previous results that indicated a hydrophobicity dependent increase of the binding capacity to flavan-3-ol. The titration of poly(L-proline) with the oligomeric tannin fraction gave a thermogram, in contrast with the monomers, in which the peaks were exothermic and became endothermic once all binding sites were saturated. This observation was explained with cooperative binding and

bridging between macromolecules. Data analysis, using a one-site model, gave increasing binding constants in the order epigallocatechin gallate < epicatechin gallate < oligomeric tannins, with magnitudes in an approximate 1:2:10 relationship. Furthermore, data indicated that the formation of aggregates required much more ligand than necessary for simple binding site saturation. In addition, the formation of large aggregates between proline rich proteins and catechins requires much more ligand than required for the simple saturation of binding sites.[34]

The fact that aged wine is noted as less astringent and involved mechanisms were studied by McRae *et al.*[35] As tannin concentrations have been observed to be similar in aged and young wine, changes in astringency change seem to be dependent on structural changes of these type of compounds. Therefore, ITC experiments were carried out to determine the interactions between poly(L-proline) and tannins isolated from grape seed and skin (Fig. 2D), as well as from two- up to ten-year-old Shiraz wine. The titration curves obtained from ITC experiments were analysed using a set of identical-binding-sites model, divided into two parts. In the first one, hydrophobic interactions with large ΔH values were most pronounced for grape tannins with molar ratio less than one. These values decreased in the order from young wine tannins > grape tannins > aged wine tannins. The second part of the curve showed an increasing endothermic component, which was consistent with hydrophobic interactions resulting in the displacement of water molecules, and molar ratios greater than one. At molar ratios higher than 1, the formation of metastable aggregates was observed. These results were indicative for structure-dependent differences in the mechanism the tannins bound to poly(L-proline), and for the incorporation of anthocyanins into their structure in aged wine. The latter results in a less structured hydration shell around the compound and reduces interaction with poly(L-proline). Furthermore, intramolecular associations of the larger, more compact, and more oxidized tannins in aged wine hinders the number of binding sites available for poly(L-proline)-association. As a conclusion, these data indicated the formation of structure-dependent tannin–poly(L-proline) complexes, in a next step the aggregation of these complexes, and, subsequently, the formation of aggregate coalescence and precipitation, resulting in a lower complexation capacity of tannins to poly(L-proline) over time.[35]

Antioxidant and Anticancer Activity of Polyphenols.
Antioxidant activity of polyphenols has found wide application in radioprotection and cancer prevention by scavenging reactive oxygen species. Enzyme inhibition showed to be involved in the responsible mechanisms. In the investigation carried out by Pal *et al.*[36], the thermodynamic parameters recorded for the binding of epicatechin, epigallocatechin, epicatechin gallate, and epigallocatechin gallate (Fig. 2B and C) with catalase resulted in negative heats with binding constants between 1.9 and 8.2×10^5 M^{-1}, emphasizing that the interactions of all four catechins with catalase are spontaneous and exothermic. The favourable ΔH values between -1.88×10^3 and -3.06×10^5 kJ mol^{-1}, and unfavourable $-T\Delta S$ values from 6.19 to 1.00×10^5 kJ mol^{-1} showed the implication of hydrogen bonding and

electrostatic contributions with polar groups of the protein and the galloyl moiety. Thus, ITC data indicate that the anticancer activity of the evaluated compounds is mainly due to catalase inhibition.[36]

With the objective to determine the inhibitory effect of flavonoids on xanthine oxidase (XOD), Tung *et al.*[37] investigated the interaction of five major flavonoids, (−)-2,3-*cis*-3,4-*cis*-3,3',4,4',7,8-hexahydroxyflavan, (−)-2,3-*cis*-3,4-*cis*-4'-methoxy-3,3',4,7,8-pentahydroxyflavan, melanoxetin, transilitin, and okanin (Fig. 3A–C), from *Acacia confusa* heartwood extracts by ITC. The results indicated an exothermically driven flavonoid–XOD interaction. Melanoxetin showed a potent inhibitory effect on XOD in a competitive mode with allopurinol. Determination of enzyme kinetics and comparison of Michaelis constants K_m of XOD with xanthine, allopurinol, and melanoxetin (values of 21.0, 24.5 and 34.6 µM, respectively) showed that melanoxetin possess an inhibitory effect superior to that of clinically used allopurinol, so that the antihyperuricemic effect of melanoxetin could be similar.[37]

Hydroxycinnamic acids and their quinic acid derivatives (CHA) exhibit a wide range of biological activities, including antioxidant. The aim of the study carried out by Budryn *et al.*[38] was to characterize the stability and degree of interaction, as well as the pH and temperature dependence of green coffee extracts and β-cyclodextrin-bound CHAs with different commercially available protein formulations commonly used in food industry. The binding degree was determined by liquid chromatography and mass spectrometry. ITC studies were used to determine the thermodynamic parameters and were carried out in aqueous solution instead of buffer to avoid the participation of ions in the active sites of the proteins. The number of binding sites for 5-caffeoylquinic acid (5-CQA),
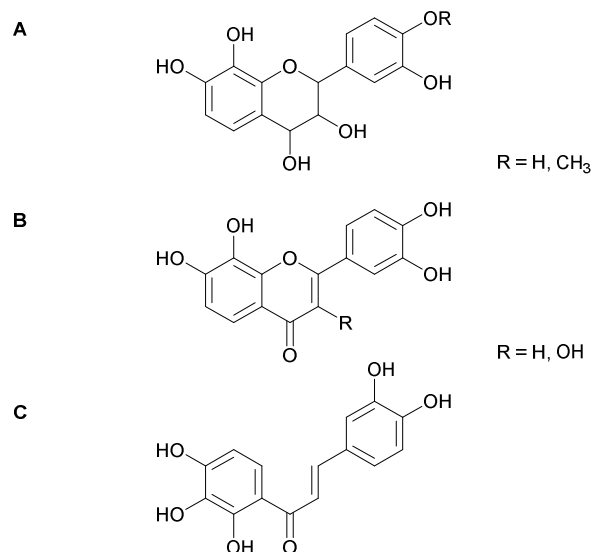
Fig. 3 Polyphenolic compounds from *Acacia confusa* heartwood investigated for their inhibitory activity of xanthine oxidase (A–C) and from *Rheum* sp. evaluated as inhibitor of retinoic X receptor (D). **A**, (−)-2,3-*cis*-3,4-*cis*-3,3',4,4',7,8-hexahydroxyflavan (R=H) and (−)-2,3-*cis*-3,4-*cis*-4'-methoxy-3,3',4,7,8-hexahydroxyflavan (R=CH₃); **B**, transilitin (R=H) and melanoxetin (R=OH); **C**, okanin.
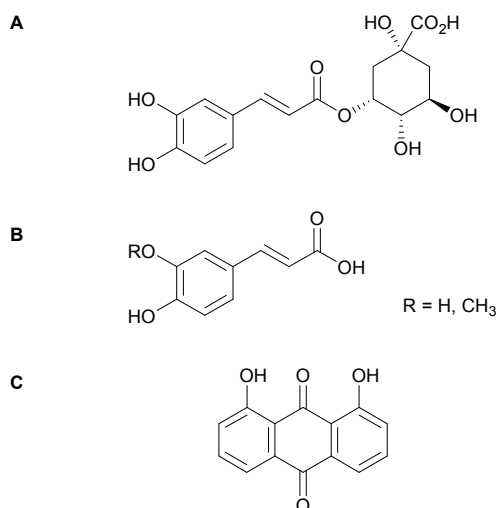
Fig. 4 Compounds mentioned in the text that have been evaluated for their protein binding. **A**, 5-*O*-caffeoylquinic acid; **B**, caffeic acid (R=H) and ferulic acid (R=CH₃); **C**, 1,8-dihydroxyanthraquinone (danthron)

caffeic acid (CA), or ferulic acid (FA) (Fig. 4A and B) with whey protein concentrate (WPC), egg white proteins (EWP), and soy protein isolate (SPI) evaluated by ITC resulted in binding ratios between 2.12 (WPC–CA) and 32.8 (SPI–CA). The ΔH values in the range between -2.43 kJ mol^{-1} for SPI–5-CQA and -146 kJ mol^{-1} for WPC–CA, and $-T\Delta S$ values from -5.25 (WPC–5-CQA) to -23.85 (SPI–5-CQA) kJ mol^{-1} showed that the interactions were hydrophobic, non-covalent, and suggested to be stabilized by hydrogen bonding. Except for WPC–CA-binding ($-T\Delta S$ 126.12 kJ mol^{-1}), interactions were entropy driven with possible implication of hydrogen bonds. In addition, in contrast to the other evaluated complexes, binding of CA and EWP was endothermic, suggesting conformation changes upon CA binding. The obtained binding constants ranged from 1.93 to 39.4 × 10^3 M^{-1}. The highest binding values were obtained in SPI, which confirmed that this protein had the largest amount of binding sites. In conclusion, the interactions of caffeic, ferulic, and chlorogenic acids from green coffee beans with food proteins were strong, whereas β-cyclodextrin bound phenolic acids showed limited binding.[38]

Retinoic X receptor (RXR) has been revealed as an important target in the treatment of cancer and metabolic syndromes. However, there is little knowledge on the structural requirements of RXR antagonists. To get deeper insights into these type of interactions, the binding of 1,8-dihydroxyanthraquinone (danthron, Fig. 4C), obtained from the traditional Chinese medicine rhubarb (*Rheum* sp.), to RXRα-ligand binding domain (LBD), as well as its influence on corepressor SMRT binding, was evaluated by ITC by Zhang *et al.*[39] The obtained results were in contrast to previously published data obtained by methods other than ITC[51–53] and indicated that danthron binds to the receptor in a ratio of 1:2. This result was confirmed by the danthron-soaked crystal structure of tetrameric RXRα-LBD. The dissociation constant of danthron–RXRα-LBD was 7.5 μM. Furthermore, danthron

binding stabilized tetrameric RXRα-LBD and affected the corepressor SMRT affinity to to RXRα-LBD, although the involved mechanism was not clear.[39]

Polyphenol Drug Distribution. Drug distribution in the blood stream depends on various factors, being the binding to serum proteins, such as albumins, of importance. Several ITC studies on the interaction of bovine serum albumin (BSA) and flavonoids are available.[40–43] The studies of Frazer *et al.*[40,41] focused on the interaction between epicatechin (EC, Fig. 2B) and BSA and showed that binding is exothermic (ΔH values between -37 and -61 kJ mol^{-1} for 0.05, 0.2, and 0.5 mM BSA), weak (K_d values between 107 and 291 M^{-1} for 0.05, 0.2, and 0.5 mM BSA), non-covalent, and unaffected by pH changes. Electrostatic interactions showed not to be a major factor in the formation of the EC–BSA complex. A comparative ITC experiment for the interaction of EC and gelatin, which is rich in hydrophobic proline residues, suggests that the binding of EC is likely to depend on hydrogen bonding and not on hydrophobic forces.[41] In addition, comparison of binding isotherms of gallotannins and ellagitannins to BSA (Fig. 5A–C) obtained in a previous study[40] suggest that epicatechin non-specifically adsorbs onto the surface of the BSA, which leads to protein aggregation and eventual precipitation.
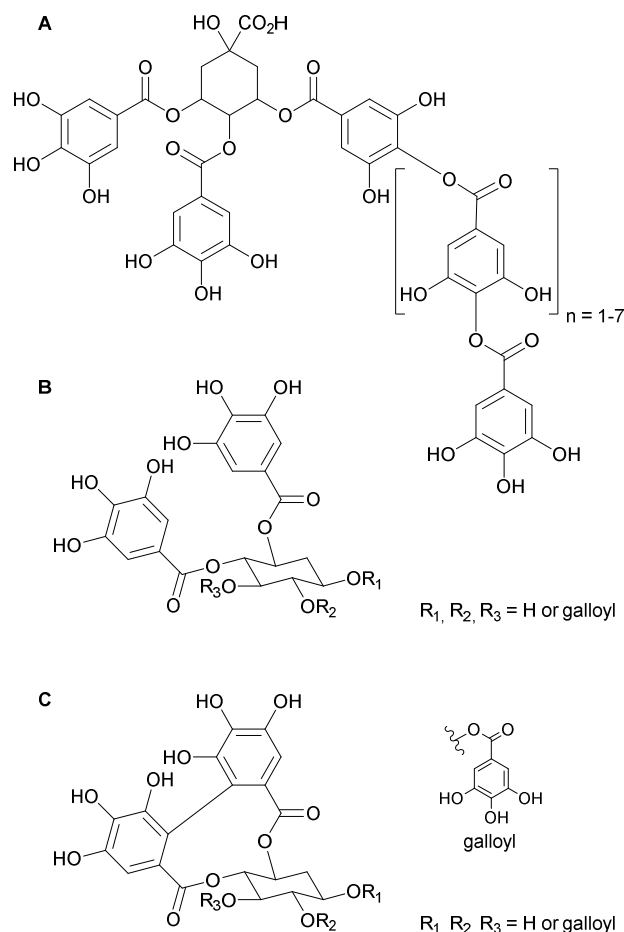
Fig. 5 Polyphenols that have been evaluated by ITC for their binding to bovine serum albumin. **A, B,** gallotannins; **C**, ellagitannins.
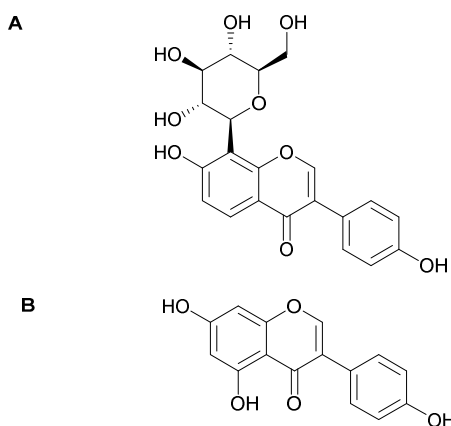
Fig. 6 Polyphenols evaluated by ITC for their implication in drug transport (A) and amyloidoises (B). **A**, puerarin; **B**, genistein.

ITC studies of the interaction of epicatechin (EC) and epicatechin gallate (ECG) (Fig. 2B and C) with BSA carried out by Pal et al.[42], showed negative heats (−4.05 and −2.57 kJ mol^{-1}, respectively) with binding constants of 9.7×10^4 and 27×10^4 M^{-1}, respectively. The negative ΔG values (−28.45 and −30.96 kJ mol^{-1}, respectively) indicated a spontaneous and entropy-driven binding process, as contribution of $-T\Delta S$ with values of −24.27 and −28.45 kJ mol^{-1} for EC and ECG, respectively, was significant. In contrary to EC–BSA interaction, ECG–BSA complexation was strong and hydrophobically driven, with the implication of electrostatic interactions. These data indicated that the galloyl moiety contributes substantially to a higher binding efficiency of ECG to BSA.[42]

ITC data obtained by Xi et al.[43] for the interaction of puerarin (Fig. 6A), a naturally occurring isoflavone C-glycoside, to BSA showed negative heats in the range of −5.27 and −0.54 kJ mol^{-1} and negative $-T\Delta S$ values (from −201.00 to −95.17 kJ mol^{-1}) at temperatures from 293 to 308 K. Furthermore, the results indicated a burial of hydrophobic groups due to the binding process, as well as the induction of a conformational change in albumine, which was further proved by the analysis of CD- and FT-IR spectral data.[43]

Role of Polyphenols in Amyloidoises. Aggregation of amyloid β-protein, which converts from its soluble random coil form into β-sheet-rich fibrils, is a characteristic landmark of neurodegenerative Alzheimer's disease. In this context, amyloid β-protein 42 (Aβ42) is considered one of the mayor factors involved in this disease due to its strong neurotoxicity and aggregation capability. Therefore, the thermodynamic characteristics of amyloydoises-related protein aggregations in dependence of natural products has been in the focus of several studies.[44–46] Wang et al.[44,45] studied the interaction of Aβ42 and Aβ42 fragments with epigallocatechin gallate (EGCG, Fig. 2C), which has been proved to be effective in reducing Aβ deposition and preventing its aggregation *in vitro*. The ITC results showed that ΔH (2.09 kJ mol^{-1} for Aβ42, and values between −17.80 and 17.22 kJ mol^{-1} for the fragments), $-T\Delta S$ (−35.12 kJ mol^{-1} for Aβ42, and −47.22 to −8.98 kJ mol^{-1} for

the fragments), as well as hydrogen bonding and hydrophobic interactions showed strong dependency on protein fragment type and size.[36] Furthermore, ΔH (−30.78 to −13.58 kJ mol^{-1} for Aβ42) and $-T\Delta S$ values (−8.68 to 6.17 to kJ mol^{-1} for Aβ42) depended on solution environment (0–200 mM NaCl), as hydrophobic interactions and hydrogen bonding changed oppositely, whereas ΔG values between −22.96 and −24.65 kJ mol^{-1} for Aβ42 were independent due to a significant enthalpy/entropy compensation.[44] In addition, as there are no specific interactions and ΔG change is insignificant with the change of the solution environment, epigallocatechin gallate binding to Aβ42 could happen over a broad range of solution conditions. Although hydrophobic interactions and hydrogen bonding are involved in the interaction between Aβ42 and EGCG, the overall data indicated that the compounds mainly act at different regions of the protein.[45]

Transthyretin (TTR) is a tetrameric thyroxine-binding amyloidogenic protein. Dissociation and subsequent misassembly of partially unfolded monomers into amyloid fibrils, amorphous aggregates, and subsequent deposition is involved in several severe amyloid diseases, such as senile systematic amyloidosis, familial amyloid polyneuropathy, familial amyloid cardiomyopathy, and central nervous system amyloidosis. In the ITC studies of Trivella et al.[46] and Green et al.[47], the dissociation constants ($K_{d1} = 0.04$ μM and $K_{d2} = 1.4$ μM) of the TTR–genistein complex indicated that genistein (Fig. 6B) exhibited strong aggregation inhibition at equal concentrations of genistein and TTR, bound with negative cooperativity, and kinetically stabilized TTR under both native and denaturing conditions. Thus, this compound resulted an excellent acid-mediated TTR amyloidogenesis inhibitor.[46,47]

Role of Polyphenols in Antibiotic Resistance. A major mechanism of antibiotic resistance in bacteria is the active extrusion of toxic compounds through membrane-bound efflux pumps. In this context, the TtgR protein, that contains two distinct, overlapping ligand binding sites for effectors and DNA, represses the transcription of efflux pump TtgABC in a *Pseudomonas putida* line. Antibiotics, e.g. chloramphenicol (Fig. 7A), and plant secondary metabolites, such as naringenin and phloretin (Fig. 7B and C), are known to bind to the effector TtgR, which results in an increase of TtgABC expression and reduce antibiotic resistance. The thermodynamics of this phenomenon was investigated in the study of Daniels et al.[48] One wildtype and five mutant TtgR proteins were used to determine their binding to the effectors naringenin, phloretin, and chloramphenicol and to quantitate the effects of mutated amino acid residues within the effector's binding pocket. The obtained results showed that the thermodynamic modes of binding were enthalpy driven, with negative ΔG values between −34.98 and −33.18 kJ mol^{-1} for phloretin, −31.88 and −29.71 kJ mol^{-1} for naringenin, and −30.79 and −27.53 kJ mol^{-1} in the six tested proteins, including no binding of chloramphenicol in some cases. Comparison of the obtained K_d values for compound binding to the six tested proteins, ranging from 0.93 to 1.90 μM for phloretin, 3.22 to 7.52 μM for naringenin, and 4.91 to 17.86 μM for chloramphenicol, enabled the
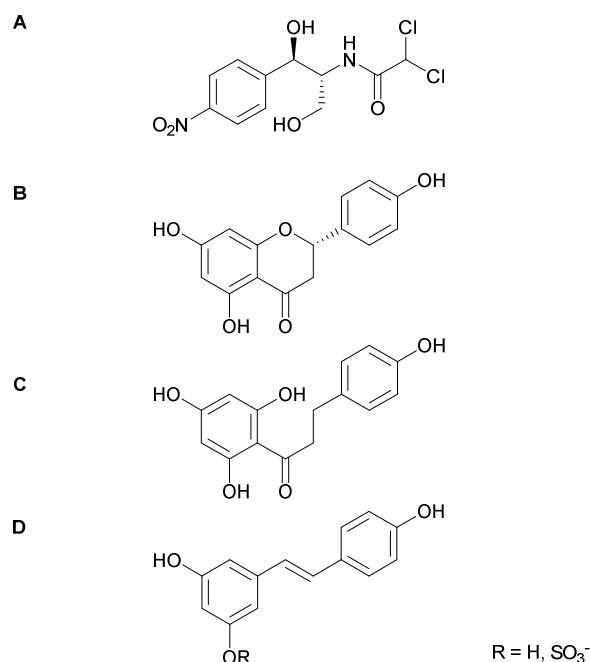
Fig. 7 Polyphenols involved in antibiotic resistance (A-C) and diabetes (D). **A**, chloramphenicol; **B**, naringenin; **C**, phloretin; **D**, resveratrol (R=H) and resveratrol-3-sulphate (R=SO₃⁻).

conclusion that, in most of the cases, chloramphenicol binding depends considerably on the the type of the mutation, whereas flavonoid binding was not significantly modified. These data, in combination with structural analyses, *in vitro* and *in vivo* studies, evidenced inter-domain communication and showed that several of the targeted amino acid residues within the effector binding pocket are required for both effector and DNA binding.[48]

Polyphenols in Diabetes. MitoNEET is a mitochondrial membrane protein that is known to bind the antidiabetic drug pioglitazone, however the physiological role of this protein is unknown. In the search for new binding partners, Arif *et al.*[49] found that resveratrol-3-sulfate (Fig. 7D) formed complexes with MitoNEET, while resveratrol (Fig. 7D) showed no interaction by ITC. A stoichiometry of four molecules was observed for the binding with the monomeric form of the protein in a sequential fashion being, which was consistent with observations made by mass spectrometry. Dissociation constants were in the range of 5–16 μM for the four binding sites, and enthalpy (ΔH between -0.64 and -5.21 kJ mol^{-1}) and entropy changes ($-T\Delta S$ between -27.14 and -23.34 kJ mol^{-1}) were favourable. These results provided new information about the mode of action of resveratrol metabolites and show that resveratrol derivatives may account for the same biological effects as the natural product, combined with a better metabolic profile.[49]

2.2 Interaction of Proteins with Amines, Amides and Peptides

The transcription termination factor rho is an ATP-dependent hexameric helicase that terminates RNA transcripts in bacteria.

The natural product bicyclomycin (BCM, Fig. 8A) is a commercial antibiotic and inhibits rho as reversible, non-competitive inhibitor of ATP hydrolysis. However, the deduced low binding affinity of the bicyclomycin–rho complex, as indicated by *in vitro* kinetic assays (K_i 21 μM for ATP hydrolysis) and low rho solubility are responsible for the experimental limitation to evaluate this interaction. In an ITC study, in combination with MS and X-ray crystallographic studies, Brogan *et al.*[54] followed a technique described for low affinity systems[10] titrating BCM into a rho solution (24 μM rho, based on monomer) containing poly(dC) (1.33 μM) and ATP (200 μM). The limited experimental data indicated that rho–BCM interaction ($K_d \approx 40$ μM, Wiseman c value 0.6) was entropy driven (ΔH -3.31 kJ mol^{-1}). However, in order to make this interaction experimentally more accessible, a novel technique using reversible covalent imine formation with rho was applied. Thus, BCM derivatives were evaluated in a poly(C)-dependent ATPase assay to select a suitable candidate for an ITC study. The obtained thermodynamic data for 5α-(3-formylphenylsulfanyl)-dihydrobicyclomicin (Fig. 8B) showed that its interaction with rho (K_d 2.5 μM with ATP and
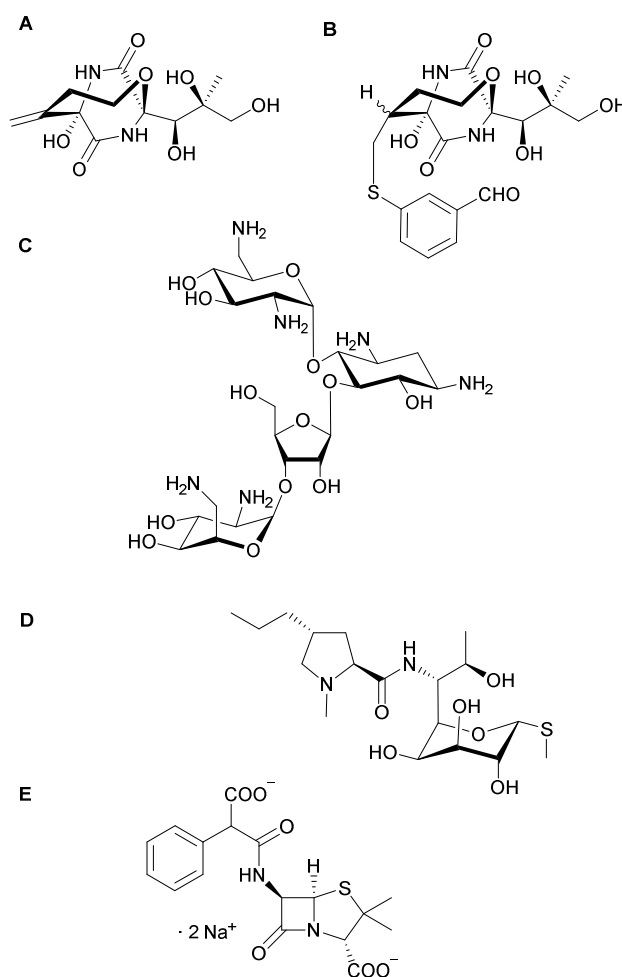
Fig. 8 Antibiotics of natural origin used in ITC assays. **A**, bicyclomycin; **B**, 5α-(3-formylphenylsulfanyl)-dihydrobicyclomicin; **C**, neomycin; **D**, lincomycin; **E**, carbenicillin.

6.3 μM without ATP) is an order of magnitude more efficient than in the rho-BCM complex. In addition, the interaction of the derivative with rho showed to be enthalpy driven, and ATP presence showed no appreciable effect on binding (ΔH −11.46 and −5.61 kJ mol^{-1} with or without ATP, respectively). The larger ΔH observed for the analogue was deduced to depend on the thermodynamics of imine bond formation with rho. The binding stoichiometry of 6 showed that the BCM derivative binds equally to all six rho hexamers in presence and absence of ATP. This observation was even more surprising as ATP binding to the nearby ATP binding pocket was homogeneous.[54]

Neomycin and lincomycin (Fig. 8C and D), two antibiotics of the aminoglycoside and lincosamide family, have been tested for their interaction with bovine (BSA) and human serum albumins (HSA). ITC data obtained by Keswani et al.[55] at temperatures between 288.15 and 308.15 K showed that neomycin binding to BSA and HSA was weak (0.78–1.27 × 10^3 M^{-1}), enthalpically favoured (ΔH −30.54 kJ mol^{-1} and −30.30 kJ mol^{-1} at 298.15 K for BSA and HSA, respectively), entropically opposed (−$T\Delta S$ 13.10 kJ mol^{-1} for BSA and 14.01 kJ mol^{-1} for HSA at 298.15 K), and with a 1:1 binding stoichiometry. At temperatures above 298.15 K, binding becomes more exothermic and with a larger unfavourable entropy compensation. In addition, burial of hydrophobic residues upon ligand binding showed to contribute to the interaction, as shown by the negative value of heat capacity of binding. The authors found a divergence between their calorimetric results and the calculated van't Hoff enthalpy that was interpreted as a result of protein conformational changes upon ligand binding. However, the difficulties in finding an appropriate fitting model and the large deviations observed in ΔH^o values recorded at high temperatures suggest that, alternatively, the divergence may also be explained by the fact that different species were tested. Furthermore, the analysis of the effect of presence of tetrabutyl ammonium bromide and surfactants indicated electrostatic predominance in neomycin–serum albumin interaction. These data were consistent with those obtained for the interaction of carbenicillin (Fig. 8E), a semisynthetic β-lactam antibiotic, with BSA.[56] In contrary to ITC data obtained for neomycin, lincomycin did not show any evidence for binding to serum albumins in their native state, but rather interacts in the presence of surfactants. The calorimetric results have been coupled with spectroscopic observations.[55]

Human cyclophilin 18 (hCyp18) from the peptidyl prolyl cis/trans isomerase (PPIase) family, is the major cytosolic receptor for cyclosporin A (CsA, Fig. 9A), a clinically used cyclopeptide for immunosuppression. Formation of hCyp18–CsA-complex is essential for CsA activity. To bring light on the great variety of reported dissociation constants (1.6−5000 nM), hCyp18–CsA interaction was investigated by Fanghänel and Fischer[57] using ITC, performing a reverse titration of a low solubility CsA solution (2–6 mM) within the sample cell and hCyp18 within the injection syringe. Although CsA and the binding pocket of hCyp18is are hydrophobic, binding at 289.0 K was enthalpy driven (ΔH values between −77.82 and −61.50 kJ mol^{-1}) and entropically unfavourable (−$T\Delta S$ between 15.48
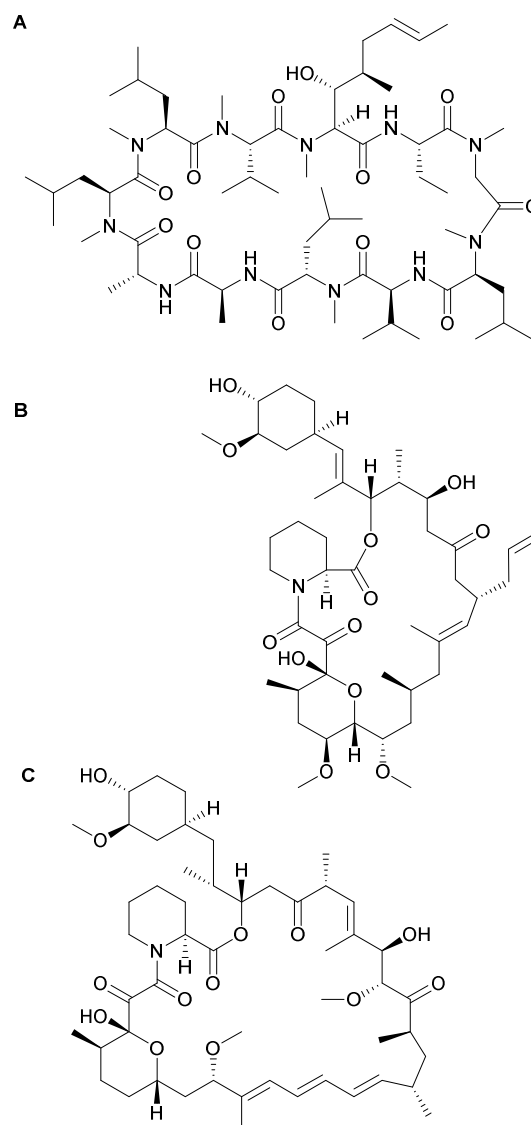

Fig. 9 Macrocyclic antibiotics of natural origin used in ITC assays. **A**, cyclosporin A; **B**, tacrolimus (FK506); **C**, rapamycin.

and 32.64 kJ mol^{-1}). The dissociation constant (K_d 9.09 nM) was in close agreement with the reciprocal of an experimental inhibitory constant of the PPIase activity of hCyp18. Enthalpy/entropy compensation resulted in an almost unaffected ΔG value over the temperature range investigated, while ΔH and −$T\Delta S$ were strongly linear temperature-dependent. Further interpretation of the thermodynamic parameters in buffered solution of water, 30% glycerol, and deuterium oxide (D$_2$O) let conclude that CsA–hCyp18 interaction is mainly mediated through hydrogen bonding and, in a certain degree, through hydrophobic interaction. In addition, sequestered water molecules play an important role in the interaction, confirming previous conclusions by interpretation of reported crystal structures. Moreover, an isotope effect was observed, as the binding constant increased significantly in D$_2$O over the entire temperature range examined. Binding constants of hCyp18–CsA

interactionshowed low sensitivity to temperature (between 5 and 33 °C) or buffer composition. However, experiments carried out at pH between 5.0 and 8.2 showed a pH dependent binding process. Under all conditions, the calculated binding stoichiometry was 1:1, indicating that no additional low affinity binding sites should be implicated. Thus, the catalytic pocket of hCyp18 should be the CsA binding site.[57]

Comparing data obtained for the CsA–hCyp18 interaction with those from Conelly *et al.*[58] for the interaction of another PPIase, FKBP12, with the immunosuppressors tacrolimus (FK506) or rapamycin (Fig. 9B and C) in D_2O, it turned out that rapamycin–*h*FKBP12 interaction was less exothermic in heavy water over the range of temperature examined and did not affect FK506–*h*FKBP12 interaction. The change in ΔH was ascribed to a transfer of non-polar compounds from H_2O to D_2O, which was also observed in the CsA–hCyp18 interaction and seemed to be overcompensated at higher temperatures by the favourable enthalpic contribution of stronger hydrogen bonds in D_2O. These results indicate that the modes of PPIase interaction in CsA–hCyp18 and FK506–hFKBP12 are different and that water play an important role in the tight interaction of CsA and *h*Cyp18.[58]

2.3 Protein–Alkaloid Interactions

Polymerization and depolymerization of contractile actin stress fibers play a crucial role in cell motility and is implicated in various physiological and pathological cellular processes, as well as malignancies, such as cancer metastasis and chronic inflammation. Sceptrin (Fig. 10A), a bioactive bromophyrrole alkaloid from a marine sponge, has been described to interact with bacterial MreB protein, the bacterial actin homologue. The potential application of this natural product as actin-dependant cell motility inhibitor has been evaluated by different *in vivo* and *in vitro* methods. In this context, the ITC study of Cipres *et al.*[59] on its interaction with G actin showed that sceptrin was able to bind mammalian monomeric actin with an equilibrium dissociation constant K_d of 19.2 ± 0.2 μM, which could be one explanation for the compound's effect on cell contractility.[59]

Sanguinarine, a quaternary benzophenanthridine alkaloid present in many plants, presents various biological activities, including induction of apoptosis in cancer cells. The interaction of its iminium and alkanolamine forms (Fig. 10B) with serum albumins may play a critical role in toxicity and biodistribution of this natural product. The ITC study of Hossain *et al.*[60] showed that sanguinarine binding to BSA was exothermic with strong enthalpy/entropy compensation. However, the iminium binding was enthalpy driven (ΔH −25.73 kJ mol^{-1} and $-T\Delta S$ −1.34 kJ mol^{-1} at 298 K), indicating a stronger electrostatic interaction, whereas the binding of the alkanolamine was favoured by strong entropy contribution (ΔH −10.71 kJ mol^{-1} and $-T\Delta S$ −21.46 kJ mol^{-1} at 298 K), which was indicative of a predominant hydrophobicity effect. The binding constants were determined as 7.95 × 10^4 M^{-1} and 37.8 × 10^4 M^{-1} (298 K), respectively. The non-linear temperature dependence for BSA–alkanolamine complex could be a contribution of linkage
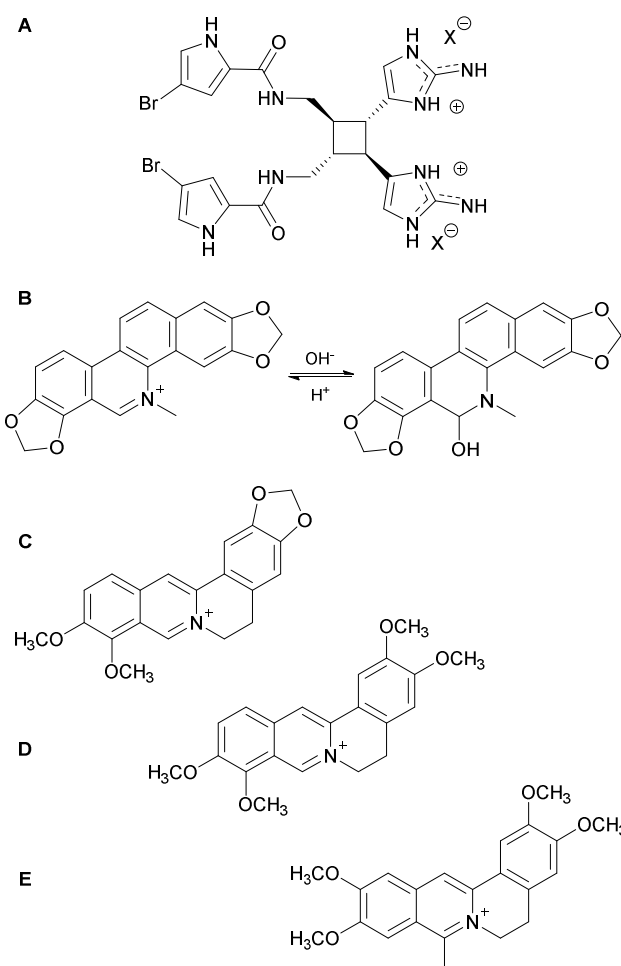
Fig. 10 Alkaloids evaluated by ITC for their protein binding ability. **A**, sceptrin (X=Cl, AcO, TFA); **B**, sanguinarine, iminium (left) and alkanolamine form (right); **C**, berberine; **D**, palmatine; **E**, coralyne.

interactions or conformational changes during the binding process, confirming previous observations by circular dicroism studies. The calculated number of binding sites was higher for the iminium ($n \approx 0.3$) than for the alkanolamine form ($n \approx 0.2$). These results show that binding to serum albumin is more favoured for the alkanolamine form than for the charged iminium form.[60]

Another serum protein implicated in drug distribution is human haemoglobin (Hb). In order to be able to understand the involved mechanisms for effective blood distribution of isoquinoline alkaloids, Hazra *et al.*[61] studied the binding characteristics of haemoglobin to berberine, palmatine, and synthetic coralyne (Fig. 10C–E) by ITC in combination with other calorimetric and spectroscopic techniques. Isoquinoline–Hb–interaction was observed to be an exothermic process with a 1:1 binding ratio. The binding affinity at 25 °C increased in the order coralyne > palmatine > berberine (K_d 8.70, 11.49 and 15.38 μM, respectively). The interaction of all three compounds with Hb were characterized to be favoured by enthalpy (ΔH between −20.17 and −5.31 kJ mol^{-1}, −19.75 and −5.19 kJ mol^{-1}, and −19.20 and −6.40 kJ mol^{-1} between 15 and 35 °C

for berberine, palmatine, and coralyne, respectively) and entropic changes ($-T\Delta S$ values between -23.51 and -6.36 kJ mol^{-1} for all three compounds between 15 and 35 °C). The evaluation of temperature dependency showed a decrease in affinity at higher temperature with more negative binding enthalpy values. These observation showed a dominant entropy contribution at lower temperatures and a strong enthalpy/entropy compensation. The analysis of heat capacity changes (ΔC_p -0.74, -0.73, and -0.64 kJ mol K^{-1} for berberine, palmatine, and coralyne, respectively) indicated specific binding with burial of the non-polar surface area for all three compounds. In addition, negative heat capacity is responsible for a shift from the entropy dominated binding at low temperatures to an enthalpy dominated one at higher temperatures. The overall data indicated the implication of strong hydrophobic interactions along with electrostatic interactions with the charged isoquinolines, inducing structural changes in haemoglobin structure.[61]

2.4 Protein–terpene interactions

Testosterone, the major androgen in humans, is responsible for related disorders in men and women. Diagnosis and treatment is based on the measurement of the levels of circulating free testosterone (FT, Fig. 11A) in blood. As available assays are too complex and often with poor reliability, levels of FT are calculated on the basis of total testosterone, albumin, and sex hormone binding globulin (SHBG) levels. However, calculated values do not match very well to those obtained by randomized testosterone trials in men and women. In the search for a more reliable method to measure FT, Zakharov *et al.*[62] evaluated the molecular basis of this discrepancy by equilibrium dialysis, ligand depletion curves, ITC, and comparison of the obtained results with different existing binding models. The binding isotherm for the titration of SHBG at three concentrations with testosterone displayed two saturation plateaus and asymmetry at values near the EC$_{50}$ value. These observations could not be reproduced by theexisting models, but were explained with good fit by a new model with complex allostery, as shown in Fig. 11B. This new model based on ITC data was validated by equilibrium dialysis in men and women and showed no statistical difference.[62]

The plant terpenoid paclitaxel (Fig. 11C) is a clinically used anticancer drug, which acts as a microtubule stabilizing agent. These types of drugs were proposed to protect from β-amyloid toxicity. In addition, insulin was reported to form cytotoxic fibrillar and prefibrillar intermediates similar to β-amyloid protein. Therefore, Kachooei *et al.*[63] studied paclitaxel for its effect on insulin stabilization and its action as protein fibrillation inhibitor. The ITC data of the interaction between paclitaxel and bovine insulin at acidic pH values indicated a spontaneous and enthalpy driven interaction (ΔH -474.05 kJ mol^{-1}). The stoichiometry was determined as 1.32, with a binding constant of 3.06×10^4 M^{-1}. In contrast to previous results, enthalpy and entropy changes indicated a major implication of van der Waals interactions and hydrogen bond
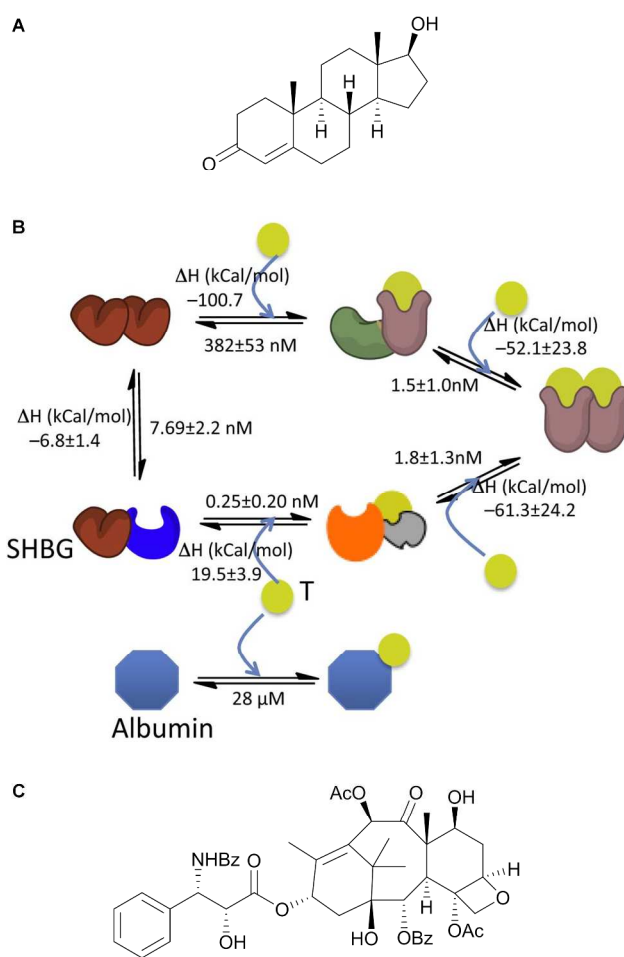

Fig. 11 Structures of terpenoids (**A, C**) mentioned in the text and the new model for the interaction of testosterone and sex hormone binding globulin (**B**). **A**, testosterone; **B**, new, ITC-based multi-step binding model of testosterone (A) to sex hormone binding globulin (SHBG).[62] Reprinted from: Molecular and Cellular Endocrinology, Vol. 399, M. N. Zakharov et al., Pages 190–200, Copyright (2015), with permission from Elsevier; **C**, paclitaxel.

formation. In combination with other spectroscopic assays and computational methods, paclitaxel at low doses was shown to reduce the formation of β-sheet structures, hindering nucleation of insulin, and reducing neurotoxicity of insulin fibrils.[63]

2.5 Interactions of Proteins with other Natural Products

The prokaryotic tubulin homolog, FtsZ, is a highly conserved protein in bacteria and has a central role in cell division. *trans*-Cinnamaldehyde (Fig. 12A) is a natural product isolated from *Cinnamomum cassia* and inhibits bacterial growth including multi-drug resistant strains. To elucidate the involved inhibition mechanism, Domadia *et al.*[64] used ITC, STD-NMR, confocal microscopy, and *in silico* molecular modelling. ITC data indicated that FtsZ–cinnamaldehyde interaction was exothermic. A high affinity binding was indicated by favourable enthalpic interactions (ΔH -47.11 kJ mol^{-1}) and a positive entropy term ($-T\Delta S$ 13.00 kJ mol^{-1} at 293.15 K). The affinity constant was 1.0×10^6 M^{-1} for a binding stoichiometry of one. The obtained results revealed that cinnamaldehyde
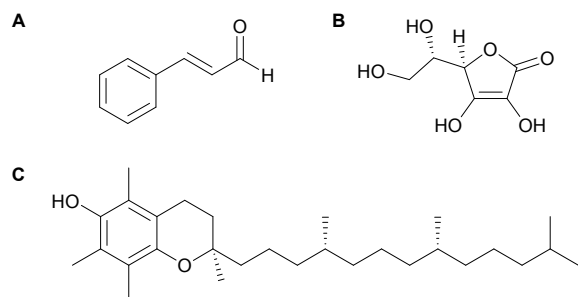
Fig. 12 Compounds mentioned in the text that have been evaluated for their protein binding using ITC. **A**, cinnamaldehyde; **B**, ascorbic acid; **C**, α-tocopherol.

inhibited GTPase dependant polymerization of FtsZ, which was confirmed by competitive binding experiments of FtsZ with cinnamaldehyde and SulA, a protein with known FtsZ inhibition mechanism, suggesting an overlap of the corresponding binding pockets.[64]

Ascorbic acid and α-tocopherol, the biologically active form of vitamin E (Fig. 12B and C), are plasma antioxidants capable of reducing the oxidative stress effects of various diseases. Although research into their *in vivo* mechanisms has been extensive, the binding mechanism of these two compounds to bovine serum albumin (BSA) has been less investigated. The thermodynamics of the binding of water-soluble ascorbic acid and lipid-soluble α-tocopherol to BSA were carried out by Li *et al.*[65] using ITC in combination with spectroscopic observations. The obtained results indicated that binding of both antioxidants to BSA is spontaneous and exothermic, driven by favourable enthalpy (ΔH_1 −71.87 kJ mol^{-1} and ΔH_2 −91.09 for ascorbic acid, and -1.27×10^3 kJ mol^{-1} for α-tocopherol) and unfavourable entropy ($-T\Delta S_1$ 41.8 kJ mol^{-1} and $-T\Delta S_2$ 67.29 kJ mol^{-1} for ascorbic acid, and $-T\Delta S$ 1232.83 kJ mol^{-1} for α-tocopherol at 298 K). The major driving forces are hydrogen bonding and van der Waals forces, as indicated by negative entropy and negative enthalpy changes. The obtained dissociation constants (K_{d1} 5.38 and K_{d2} 67.11 μM for ascorbic acid, and 1.45 μM for α-tocopherol) showed that interaction with BSA was characterized by low affinity and nonspecific binding. However, the binding mechanisms for both compounds were different, as ascorbic acid interacted through a complex multiple binding site model with negative cooperativity, whereas α-tocopherol interaction fitted to an independent-binding-site model. The obtained stoichiometry values indicated that ascorbic acid (n_1 12.8 and n_2 39.9) binding occurred by a surface adsorption mechanisms, leading to coating of the protein surface[65], which is similar to that described for BSA–flavonoid interactions.[40] In contrast, for α-tocopherol, the binding number of 0.92 suggested that one molecule combines with one molecule of BSA.[65]

Complex coacervation between oppositely charged macromolecules is a colloidal phenomenon involved in the structuring of many biological systems and is of industrial interest in the field of nanobiotechnologies or the design of biomimetic systems. In this context, to understand the thermodynamic properties of the interaction between charged proteins and polysaccharides, Aberkane *et al.*[66] studied the complexation of β-lactoglobulin (BLG) with total acacia gum (TAG) by ITC. The thermodynamic characterization in aqueous dispersion at pH 4.2 was completed by dynamic light scattering, turbidity measurements, electrophoretic mobility, and optical microscopy. During titration, the exothermic profile reversed to endothermic after 10 injections, reaching thermodynamic stability toward the end of titration. The best fit was obtained by a binding model described as a two stages structuring model, rather than by a spontaneous process. In a first step, TAG–BLG-interaction was of high affinity (K_{d1} 2.07 nM), predominantly enthalpy driven (ΔH_1 −2421.28 kJ mol^{-1}), with unfavourable entropic contributions in the same range ($-T\Delta S_1$ 2369.82 kJ mol^{-1}), and a 1:90 stoichiometry. In contrary, the second binding step was characterized by favourable binding entropy ($-T\Delta S_2$ −663.16 kJ mol^{-1}) and unfavourable enthalpy (ΔH_2 610.03 kJ mol^{-1}), indicating the prevalence of electrostatic interactions and contribution of hydrogen bonding between TAG and BLG. The temperature-independent ΔC_{p1} value (119.24 kJ mol^{-1} K^{-1}) confirmed this supposition, as its large positive value is indicative of ionization/charge neutralization reactions, and the reduction of polar surface-exposed residues. The second, entropy-driven stage was expected to be characterized by changes in intermolecular forces and conformational changes, leading to biopolymer aggregation, formation of inter-polymeric complexes, and the formation of the coacervate phase. A negative ΔC_{p2} value (-34.73 kJ mol^{-1} K^{-1}) indicated a hydrophobically driven binding process in this second stage changing the solvent-accessible surface area. Enthalpic and entropic contribution during both stages showed to be highly temperature dependent.[66]

In a similar study, Vinayahan *et al.*[67] evaluated the interaction of gum acacia (GA) and bovine serum albumin (BSA) by ITC. The results were similar to those obtained for the GA–BLG-complex, in addition to a strong pH-dependency of the interaction. Experimental data obtained at and above the isoelectric point of BSA suggested the interaction of carboxy groups on GA with positive patches on BSA. The presence of charged patches was confirmed by the observation that complexation was reduced at increasing ionic solvent strength and prevented at a NaCl concentration of 120 mM.[67]

3 Nucleotide–Natural Product Interactions

Although the classic interactions of natural products (NP) investigated by isothermal titration calorimetry focus on proteins interactions, the study of their binding to nucleotides is not less important, as many biological activities are based on nucleic acid binding. Among the NPs that are most widely investigated by ITC for their interaction with nucleotides are alkaloids. Many of the gross structural requirements for their binding activities have been elucidated up to day. However, there is still few information available on many aspects of binding specificity and binding energetics of these molecules.

In this context, the first complete thermodynamic profile of the binding of the isoquinoline alkaloid berberine (Fig. 10C) to various natural and synthetic DNAs was reported by Bhadra *et al.*[68] The results indicated that berberine–DNA binding was mostly exothermically driven and generally favoured by enthalpy and entropy change (ΔH between −135.98 and 6.53 kJ mol^{-1}, and −$T\Delta S$ between −34.18 and 115.06 kJ mol^{-1}).

The binding study of berberine to double stranded RNA polynucleotides carried out by Islam *et al.*[69] using ITC in combination with a variety of other biophysical techniques, revealed that the interaction was characterized by negative enthalpy (ΔH from −37.32 to −1.34 kJ mol^{-1}) and positive entropy changes (−$T\Delta S$ from −2.18 to 29.12 kJ mol^{-1}), except for two complexes with negative $T\Delta S$ values. These results suggested that the binding process was substantially hydrophobically driven and accompanied by enthalpy/entropy compensation, being the interaction with polynucleotides with A-U base pairs higher than those with I-C base pairs. The differentiation of the observed binding free energy values (32.64 to 36.57 kJ mol^{-1}, determined at different salt concentrations) into nonpolyelectrolytic and polyelectrolytic contributions suggested the implication of hydrophobic forces more than ionic strengths in the intercalation process due to participation of the charges on the alkaloids. Results obtained for the palmatine (Fig. 10D) were similar. The heat capacity changes for berberine, palmatine, and coralyne (ΔC_p from −1.40 to −0.23 kJ mol^{-1} K^{-1}) indicated a temperature dependent ΔH. Furthermore, the differences in ΔC_p values could indicate the release of structured water consequent to the transfer of nonpolar groups into the interior of the RNA helix. The free energy contribution from the hydrophobic transfer step (ΔG_{hyd}) of these alkaloids to the RNA structures could be calculated on the basis of the relationship $\Delta G_{hyd} = (80 \pm 10) \times \Delta C_p$. The obtained ΔG_{hyd} values in the range −112.13 to −18.41 kJ mol^{-1} were comparable to values obtained for intercalators or groove binding molecules to RNA and DNA. The overall data indicated that these compounds bind to RNA duplexes by weak partial intercalation with positive cooperativity, providing evidence for heterogeneity in the RNA conformations.[69] These results are consistent with previous data obtained for the interaction of berberine and palmatine with tRNA molecules[70,71] and further suggest that interaction of these alkaloids to DNA and RNA are similar.[68,72,73]

Cytotoxicity of the isoquinoline alkaloid sanguinarine (Fig. 10B) could be correlated with its DNA intercalation and subsequent strand breaks. In this context, the equilibrium between the charged iminium form and the neutral alkanolamine form showed strong dependency on pH values of the medium, being the iminium form responsible for DNA-binding and showing strong preference for GC base pairs and B-form DNA.[74] Various studies on the energetics of interaction with natural and synthetic DNAs in dependency of salt and pH conditions are reported in the studies of Adhikari *et al.*[75] and Hossain and Kumar[76,77]. In their studies, the thermodynamic characterization of the interaction of sanguinarine (SN) and ethidium bromide (EB), another known intercalating agent,

with CT DNA was evaluated by ITC. The results showed that binding of both drugs was exothermic and enthalpy driven (ΔH −29.25 kJ mol^{-1} and −34.47 kJ mol^{-1} at T = 293 K), with positive entropy changes (−$T\Delta S$ −4.90 and −0.77 kJ mol^{-1}), and 1.47 and 1.74 binding stoichiometries, respectively for SN and ET.[76] In addition, both alcaloids preferred purine-pyrimidine sequences, with SN showing preference for sequences with GC base pairs and ET for AT base pairs.[69] Additionally, the evaluation of SN binding to four polynucleotide sequences showed that binding was enthalpy driven (ΔH −37.82 to −18.28 kJ mol^{-1}), except for poly(dA).poly(dT) (ΔH 24.10 kJ mol^{-1}) due to its peculiar, rigid polynucleotide structure.[75]

Compared to binding studies to DNA, only few data are available concerning RNA–sanguinarine interactions. The study reported by Giri *et al.*[78] on the binding of sanguinarine (Fig. 10B) to poly(A) polynucleotides showed that this alkaloid could specifically and strongly (K_d from 0.28 to 0.22 μM) bind to this sequence. The significant positive −$T\Delta S$ value of 22.80 kJ mol^{-1} could be attributed to the formation of an ordered self-structure, and the data indicated an intercalative interaction. In comparison with berberine and palmatine (Fig. 10C and D), sanguinarine binding was stronger and, furthermore, the previously described alkaloids did not show self-structure induction in the poly(A) sequence. These results were of interest as sanguinarine could bind to the poly(A) tail of mRNA and thus represent a new type of therapeutic agent.[78]

In another study, Hossain *et al.*[79] found that the iminium form of sanguinarine (Fig. 10B) is responsible for its RNA binding. The obtained ITC data of the tRNA^{phe}–sanguinarine interaction between 10 and 25 °C indicated a binding affinity in the order of 10^5 M^{-1} for the iminium form, which was close to obtained spectroscopic data. Interaction was driven by negative enthalpy (ΔH −27.32 to −15.82 kJ mol^{-1} for 10–25 °C) and favourable entropy (−$T\Delta S$ from −17.41 to −5.46 kJ mol^{-1}). In addition, binding was characterized by a small ΔC_p value of −0.77 kJ mol^{-1} K^{-1} and enthalpy/entropy compensation.[79]

Recent ITC studies realized by Basu *et al.*[80,81] on the interaction of chelerythrine (Fig. 13A) with DNA showed that binding data of this isoquinoline alkaloid were similar to data reported for berberine, palmatidine, and sanguinarine.[82,83] To get further insights into the thermodynamic requirements of RNA binding, the interaction of the alkaloid aristololactam-β-D-glucoside (ADG, Fig. 13B) with tRNA^{phe} was investigated by Das *et al.*[84] using various biophysical techniques, and the results were compared to data obtained with daunomicin (DNM, Fig. 13C), an anticancer agent used in the clinic. The results showed that, for both compounds, binding was favoured by small negative enthalpy (−4.27 and −5.94 kJ mol^{-1}) and large negative −$T\Delta S$ values (−22.09 and −21.25 kJ mol^{-1}, ADG and DNM respectively). This observation for the interaction of DNM and RNA was in contrast to its enthalpy-driven interactions with DNA. Enthalpy/entropy compensation indicates the involvement of significant hydrophobic interactions. Furthermore, partitioning of the electrostatic and nonelectrostatic contribution to ΔG suggested that, for both ADG and DNM, electrostatic contributions are less involved in
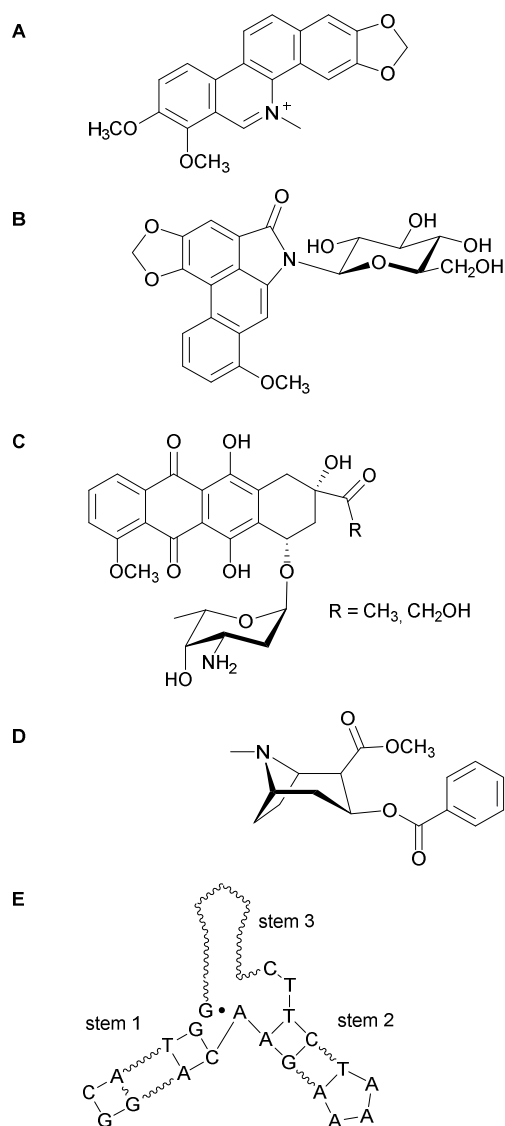
Fig. 13 Alkaloids (A–D) analyzed by ITC for their nucleotide binding affinity. A, chelerythrine; **B**, aristololactam-β-D-glucoside; **C**, daunomycin (R=CH₃) and adriamycin (R=CH₂OH); **D**, cocaine; **E**, cocaine-binding DNA aptamer used as cocaine-ligand in the ITC experiment, wavy bonds indicate modified regions.

the RNA interaction than nonelectrostatic forces. Similar results had been obtained for the interaction of isoquinoline alkaloids and RNA. However, this is contrary to the binding of many aminoglycosides to RNA, which is based on strong electrostatic interactions.[84]

The development of aptamers as biosensors or for therapeutic use is of great interest, as these compounds can exhibit highly specific ligand binding. As relatively few studies have focused on the biochemical and biophysical mechanisms implicated in the interaction, the thermodynamic insights of aptamer-ligand binding mechanisms have been investigated by Neves *et al.*[85,86] evaluating the interaction between different cocaine-binding DNA aptamer variants and cocaine (Fig. 13D and E). To be able to evaluate the weak binding, they used a low *c* ITC method and NMR spectroscopy. The results showed that two binding mechanisms are followed in dependence of the

aptamer stem length. This result was in contrast to a previously proposed mechanism.[77] When shortening of each stem, binding affinity increased, and shortening of all three stems at the same time resulted in no binding, whereas longer stems resulted in an increase of affinity.[78] All aptamer variants bound cocaine (K_d 4–204 μM) with a 1:1 stoichiometry. Binding was enthaly driven (ΔH −22.59 to −117.57 kJ mol^{-1}) and entropically unfavourable under all conditions (−$T\Delta S$ 1.05 to 88.28 kJ mol^{-1} at 293 K). A change from a GT to a GC base pair in stem3 resulted in significant tighter binding.[85] Furthermore, evaluation of the binding dependence of pH and NaCl concentration showed tightest binding at pH 7.4 and with absence of NaCl, indicating the implication of ionic interactions. Evaluation of the structural switching mechanisms showed that two separate DNA strands bound each other with a K_d of 11 μM without cocaine. This observation suggested as a result that cocaine induced folding of free DNA strands, as well as rigidifying existing DNA–DNA assemblies.[86]

Curcuminoids and flavonoids are examples for polyphenolic compounds that have been investigated by ITC for their interaction with polynucleotides. Curcumin (Fig. 14A) is known for numerous biological activities. Among them, its anticancer activity may be attributed to DNA interaction. Although there are different reports on binding mechanisms, the correspondent results are somewhat contradictory. Recently, Basu *et al.*[87] investigated the structural and energetic aspects of DNA–curcumin interaction using a spectroscopic and calorimetric based methodology. The binding was exothermic, driven by a large negative enthalpy (ΔH −18.24 kJ mol^{-1}) and a small favourable entropy change (−$T\Delta S$ −8.08 kJ mol^{-1}). K_d was determined as 24.8 μM, with 1.75 base pairs per bound curcumin, which was in agreement with the values obtained by spectrophotometry and spectrofluorimetry. Increased salt concentrations resulted in a reduced binding affinity, as well as a higher GC content was less favourable for the interaction. These thermodynamic results were in agreement with data obtained from spectroscopic studies. Analysis of the ΔG values
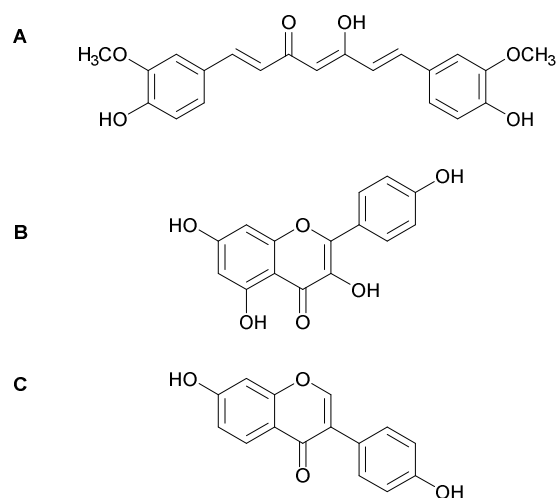
Fig. 14 Polyphenolic compounds evaluated by ITC for their polynucleotide binding. A, curcumin; **B**, kaempferol; **C**, daidzein.

and its differentiation into polyelectrolytic (ΔG_{pe} −9.08 to −5.94 kJ mol^{-1}) and nonpolyelectrolytic (ΔG_t −17.20 to −17.87 kJ mol^{-1}) forces at different sodium ion concentrations indicated that the formation of the double stranded DNA–curcumin complex was mainly hydrophobically dominated, with an involvement of forces other than electrostatic.[87]

Japanese encephalitis virus (JEV) is responsible for a central nervous system disease with irreversible neurological damage in humans. As several flavonoids have shown *in vitro* antiviral activity against a wide spectrum of viruses, Zhang *et al.*[88] investigated the capacity of flavonol kaempferol and isoflavonone glycoside daizein (Fig. 14B and C) to inhibit an α-1 translational frameshift, which is essential for the neuroinvasiveness of JEV. Therefore, the interaction between these compounds with a conserved sequence of JEV frameshift site stem-loop (fsRNA3) was evaluated by electrospray ionization mass spectrometry, docking analysis, and ITC, in order to take into consideration the influence of a structural analogy between gas-phase and solution complexes. ITC data revealed that interaction of both flavonoids was exothermic and enthalpy driven (ΔH −39.75 and −66.73 kJ mol^{-1}, respectively for daizein and kaempferol), and interaction with fsRNA3 was nine fold stronger in the case of kaempferol (K_d 11.88 nM). Moreover, it was suggested that daizein binding is due to non-covalent interactions by electrostatic and hydrophobic interactions. In the case of kaempferol, hydrogen bonding or van der Waals forces were supposed to lead to a considerable distortion of the fsRNA stem-loop structure. That way, kaempferol resulted as the more promising anti-JEV agent.[88]

Anthracycline compounds, such as adriamycin and daunomycin (Fig. 13C), are DNA topoisomerase inhibitors used in clinical treatment of highly malignant acute myeloid leukaemia. Their mechanism of action is based on intercalation, and several steps are supposed to be involved in the binding process. However, there is still few knowledge concerning the correlation of thermodynamic data with structural changes and charge neutralization during complexation. Gosh *et al.*[89] studied the interaction of these compounds with normal genomic N-DNA and mutated M-DNA from human K562 leukemic cells. To overcome aggregation problems due to the high concentration of DNA intercalator needed, the measurement was conducted as a reverse ITC experiment. For both drugs, ITC thermograms indicated exothermic binding and fitted best with a sequential binding model with four (N-DNA) or three (M-DNA) thermodynamically different binding events. This difference was explained by a conformational change during B to A transition, which is absent in M-DNA. Highest binding affinities were observed with M-DNA–daunomycin inter-actions[89], which was in accordance with earlier observations.[90] This study evidenced that mutations are able to induce changes in DNA-structure and influence drug binding efficacy.

4 Cyclodextrin–Natural Product Interactions

Host-guest complexation is an important principle in the field of sensor device development, and natural occurring

cyclodextrins (CD, Fig. 15A), cyclic oligosaccharides, are a well-known class of host compounds for the detection of organic molecules. In the study of CD–guest interactions, ITC, in comparison with a wide variety of physicochemical characterization methods, such as chromatography, electrophoresis, nuclear magnetic resonance, phase solubilisation studies, fluorescence, potentiometry, and circular dichroism spectroscopy, has shown to be a powerful method to determine binding constants and thermodynamic parameters necessary to understand the mechanisms of molecular recognition.[91]

Among the numerous guests evaluated by ITC for CD binding[91–98], bile salts are of particular interest as they are a group of physiologically important steroids with a crucial role in lipid absorption, digestion, and transportation. In this context, de Jong *et al.*[92] synthesized CD dimers and studied their potential as receptor molecules for steroid sensors with
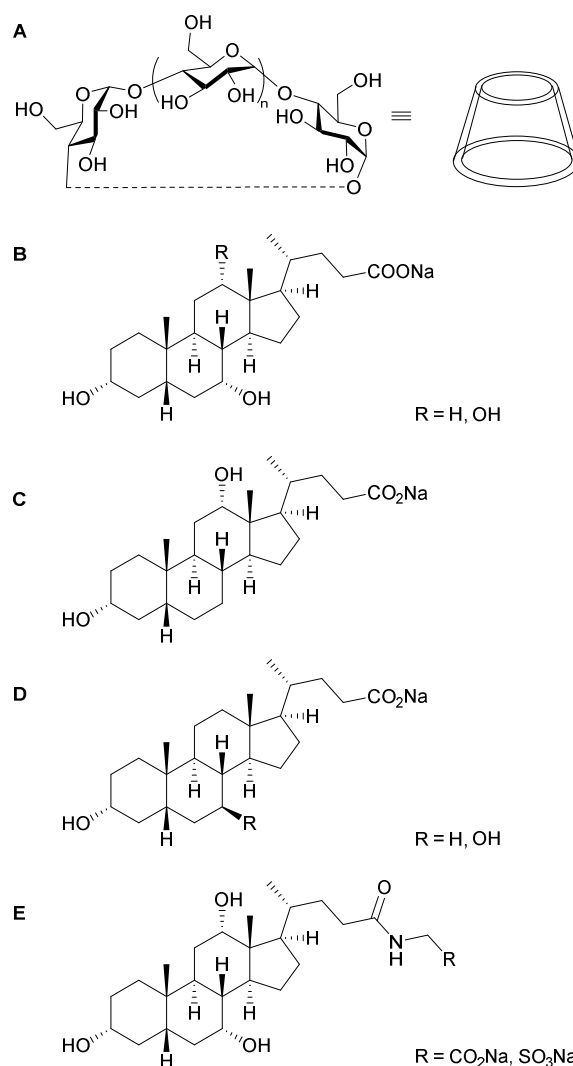
Fig. 15 Structures of bile salts evaluated by ITC for their binding to cyclodextrins (CD). **A**, cyclodextrin (n=6: α-CD; n=7: β-CD; n=8: γ-CD); **B**, cholate (R=OH) and chenodexoycholate (R=H); **C**, deoxycholate; **D**, ursodeoxycholate (R=OH) and lithocholate (R=H); **E**, glycocholate (R=CO$_2$Na) and taurocholate (R=SO$_3$Na).

increased selectivity. ITC experiments were carried out below the critical micelle concentration of the steroidal bile salts sodium cholate, deoxycholate, chenodeoxycholate, ursodeoxycholate, and lithocholate (Fig. 15B–D). The binding affinity of cholate and deoxycholate with a dipropylamino-β-CD dimer was increased by a factor of 70 and 700, respectively, relative to binding in native β-cyclodextrin (4.1×10^3 and 3.6×10^3 M^{-1}). The presence of a 12-hydroxy group in both compounds hindered deeper protrusion through one CD cavity and is followed by complexation by the second cavity, as indicated the 1:1 binding ratio. The loss of conformational flexibility in the dimer seemed to be compensated by the release of water from the cavity. On the other hand, chenodeoxycholate, ursodeoxycholate, and lithocholate showed a binding ratio of 2:1 with the dimers, as compounds could be included deeply into a single β-cyclodextrin unity. The two binding sites were identified as independent, resulting in a sequential binding behaviour. ΔH values for chenodeoxycholate (ΔH_1 −25.10 kJ mol^{-1} and ΔH_2 −30.12 kJ mol^{-1}) were less favourable than for ursodeoxycholate (−48.95 and −35.14 kJ mol^{-1}) and lithocholate (−39.33 and −37.66 kJ mol^{-1}), indicating that the fit of chenodeoxycholate in the CD cavity is less tight. In addition, the interactions showed to be dependent on the type of linker between two CD unities in the dimer. Thus, the presence of a dansyl moiety hindered the cooperation of both CD cavities necessary for cholate and deoxycholate binding, and resulted in a decrease in binding affinity (1.51×10^5 and 7.95×10^5 kJ mol^{-1}, respectively). In the case of the other steroids, this effect was less pronounced as they are strongly bound in one cavity. Apart from that, hydrophobic interactions between the steroid and the dansyl moiety were supposed to be involved in the interaction.[92]

Chen *et al.*[93] studied the molecular recognition and binding behaviour of the sodium salts of cholic acid, deoxycholic acid, glycocholic acid, and taurocholic acid (Fig. 15B, C, E, and F) with L- and D-tyrosine-modified β-cyclodextrin, using ITC in combination with circular dichroism and 2D NMR. In comparison to L- and D-tryptophan modified β-cyclodextrins, they obtained great enhancement in selectivity. This observation was due to conformational differences, which led to higher enthalpic gain and less entropic loss due to van der Waals forces, hydrogen bond, and the release of the high-energy water in the CD cavity. A binding stoichiometry of 1:1 for all compounds was deduced, and conformations of hosts and the possible binding modes were proposed by a molecular modelling study. Moreover, ITC data indicated that all interactions were driven by favourable enthalpic changes (ΔH −50.5 to −23.0 kJ mol^{-1}) attributed to strong van der Waals interactions, and unfavourable entropic changes ($-T\Delta S$ 2.4 to 27.9 kJ mol^{-1}). Although solvent reorganization upon guest binding resulted in a favourable entropic change, a large loss of conformational freedom upon host-guest binding resulted in an overall entropic loss, in consonance with an enthalpy/entropy compensation effect. Increasing binding affinities in the order deoxycholic acid > cholic acid >> glycocholic > taurocholic acid were attributed to different hydrophilic character

influencing hydrophobic interactions with the host and different volume of the side chain. On the other hand, L-tyrosine-modified β-cyclodextrin showed weaker binding to the bile salts, as D- and L-tyrosine moieties showed different self-inclusion depth into the β-cyclodextrin cavity.[93]

Triptolide (Fig. 16A), a diterpenoid triepoxide, is a potent anti-inflammatory and anticancer agent with applications in the treatment of autoimmune diseases and as immunosuppressive agent in organ and tissue transplantations. Two important limitations are its narrow therapeutic window and its low water solubility. Thus, the development of a suitable drug delivery system is of interest, in particular for oral drug formulations. As cyclodextrins (CDs) can enhance water solubility of hydrophilic compounds, Danel *et al.*[94] investigated their use as host molecules for triptolide and its 14-succinyl derivative (Fig. 16A) by separative, thermodynamic, and spectroscopic techniques at values close to physiological pH. The results of the ITC analysis of neutral hydroxypropyl-β-cyclodextrin (HP-β-CD) and cationic amino-β-cyclodextrin (A-β-CD) showed exothermic interactions (ΔH −20.08 to −10.46 kJ mol^{-1}) with both diterpenoids in a 1:1 ratio. Binding constants were determined as 128 to 336 M^{-1}, being the triptolide–A-β-CD complex the most stable one, while the HP-β-CD–triptolide complex was too weak to determine its binding strength.[94]

The improvement of the water solubility of diterpenoid paclitaxel (Fig. 11C), a microtubule-stabilizing anticancer agent used in the clinic, was the aim of Liu *et al.*[95] Their study focused on paclitaxel complexation with a series of β-cyclodextrin dimers linked with oligo(ethylenediamine) of different chain length. ITC data analysis was performed using a sequential two-step binding model. The binding constant ($K_1 \times K_2$) was calculated as 2.04×10^8 M^{-2} for a 2:1 complexation of tetraethylenepentaamino-bridged bis(β-CD) with paclitaxel. Complexation showed to be cooperatively driven by enthalpy and entropy ($\Delta H_1 + \Delta H_2$ −10.2 kJ mol^{-1}, $-(T\Delta S_1 + T\Delta S_2)$ −37.3 kJ mol^{-1}), and calorimetric data revealed the implication of van der Waals forces, hydrophobic interactions, and desolvation effects. This was surprising, as CD-binding, generally, is an
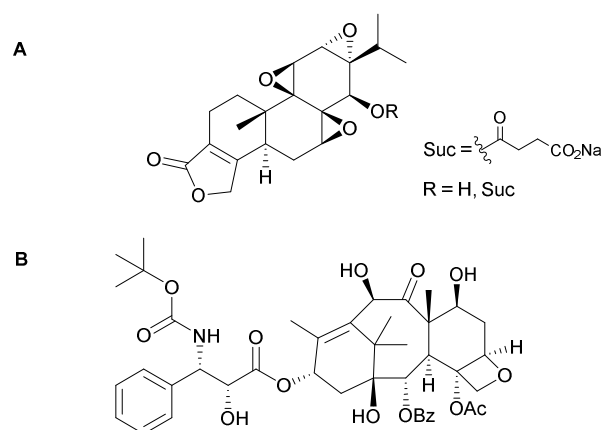

Fig. 16   **Structures of diterpenoids evaluated by ITC for their binding to cyclodextrins (CD). A**, triptolide (R=H) and derivative (R=Suc); **B**, docetaxel.

enthalpy-driven process. In addition, paclitaxel-CD complexes showed better anticancer activity than paclitaxel, in combination with an improved water solubility.[95]

Further insights into the interaction between taxanes and CDs got Mazzaferro *et al.*[96] studying the interaction of paclitaxel derivative docetaxel (Fig. 16B) and different CDs by a combination of ITC, nuclear magnetic resonance, and molecular docking studies. ITC data of the formation of docetaxel–Me-β-CD confirmed results obtained for paclitaxel.[95] Additional information was gained by the observation that the first interaction site showed a negative entropy term ($-T\Delta S_1$ -4.27 kJ mol^{-1}) with a greater hydrophobic contact surface and higher flexibility by the carbamate linker, while the second binding site showed a positive entropy term ($-T\Delta S_2$ 14.47 kJ mol^{-1}) with a restricted mobility and smaller hydrophobic contact surface. These data were coincident with molecular modelling studies and demonstrated the importance of guest flexibility in the stability of CD complexes.[96]

Application of usnic acid (UA, Fig. 17A), a natural dibenzofuran derivative isolated from lichen, in anticancer therapy is limited by its poor water solubility. Therefore, Segura-Sanchez *et al.*[97] investigated the thermodynamic characteristics of the interaction of (+)-usnic acid (UA) with α-CD, β-CD, γ-CD, hydroxypropyl-β-CD (HP-β-CD), and sulfobutylether-β-CD (SBE-β-CD) with ITC and molecular modelling. The obtained thermograms indicated exothermic heats, and best fit was obtained with a one-site binding model (1:1). Interactions were enthalpy driven (ΔH -33.50 to -14.23 kJ mol^{-1}), with negative, unfavourable entropic contribution ($-T\Delta S$ 16.31 to 0.63 kJ mol^{-1}), and enthalpy/entropy compensation. The interaction with UA decreased in the order γ-CD > HP-β-CD > SBE-β-CD > β-CD (K_d 0.97 to 6.54 mM), and no interaction occurred for α-CD. These results indicated a strong dependence of the interaction on CD cavity size, as γ-CD was able to accommodate the aromatic groups of UA, whereas α-CD could only accommodate small alkyl groups. Chemical modification of β-CD resulted in stronger binding affinity. This observations could be explained by the fact that the substitution of the hydroxy groups on the edge of the β-CD cavity by hydroxypropyl or sulfobutyl groups extend the length of the cavity and increase interaction with lipophilic regions of UA. Additionally, these modifications resulted in increased

water solubility. Variation of pH between 7 and 8 indicated an increase of complex stability at higher pH due to ionization of UA and a solubility enhancement, which was in contrast to the general observation that interactions with CD were better with more hydrophobic compounds. This was explained by molecular modelling calculations indicating the interaction of the charged moiety of UA with the hydrophobic CD cavity by means of van der Waals forces, as well as by the interaction of the negatively charged moiety of UA with the external hydroxy groups of γ-CD.[97]

Sun *et al.*[98] used ITC and NMR to evaluate the interaction of β-CD with the phenolic compounds paeonol (2-hydroxy-4-methoxyacetophone, PAE), its isomers acetovanillone (4-hydroxy-3-methoxyacetophone, ACE), and 2-hydroxy-5-methoxyacetophone (HMA) (Fig. 17B–D). The binding ratio for PAE and ACE was 1:1, and 1:1 and 1:2 for HMA. The complexation of the three compounds with β-CD showed to be a spontaneous (ΔG -37.7 to -16.1 kJ mol^{-1}), exothermic process (ΔH -9.35 to -3.06 kJ mol^{-1}), with implication of hydrophobic interactions as one of the driving forces. In addition, the binding of HMA to β-CD showed to be enthalpy driven, whereas the complex formation of the other compounds were predominantly entropy driven.[98]

5   Other Natural Product Interactions

Natural Products are known to be privileged structures able to interact with a large variety of different receptors. It is therefore not surprising that, apart from the most abundantly studied interactions described in the previous sections, ITC studies have been conducted with other receptors, including lipids[99–101], macrolides[102–106], inorganic compounds[107], and even whole cells.[108,109]

Interactions with Lipids. Witzke *et al.*[99] employed ITC, in combination with molecular dynamics simulations, to investigate the interaction of terpenoids from *Perilla frutescens* (limonene, perillaldehyde, perillyl alcohol, and deprotonated peryllic acid, Fig. 18A) with model lipid bilayers of 1,2-dimyristoyl-*sn*-glycero-3-phosphocholine (DMPC, Fig. 18B) and 1-palmitoyl-2-oleoyl-*sn*-glycero-3-phosphocholine (POPC, Fig. 18C). Their results showed negative ΔG values (-34.31 to -24.69 kJ mol^{-1}), indicative for a spontaneous partition of limonene, perillyl alcohol, and perillaldehyde into DMPC vesicles, with a much larger partition coefficient for limonene, whereas deprotonated peryllic acid showed partition problems. The effects of terpenes on POPC were similar. Thus, limonene insertion was entropy driven ($-T\Delta S$ -33.85 kJ mol^{-1} at 303 K), as this nonpolar compound had no large enthalpic interactions (ΔH -0.33 kJ mol^{-1}) with the lipid headgroups. This observation let conclude that a hydrophobic effect was responsible for insertion into the vesicles. On the other hand, perillyl alcohol insertion presents a large gain in enthalpy (ΔH -15.48 kJ mol^{-1}), which was in accordance with its polar nature, and forms hydrogen bonds with DMPC headgroups. Additionally, Perillaldehyde showed an intermediate behaviour, as it is more polar than limonene, but this compound was not
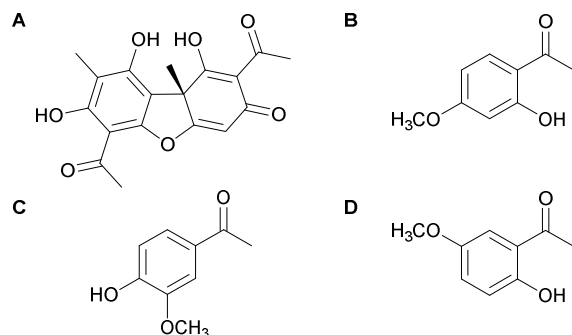

Fig. 17   Compounds mentioned in the text. A, usnic acid; **B**, paeonol; **C**, acetovanillone; **D**, 2-hydroxy-5-methoxyacetophone.
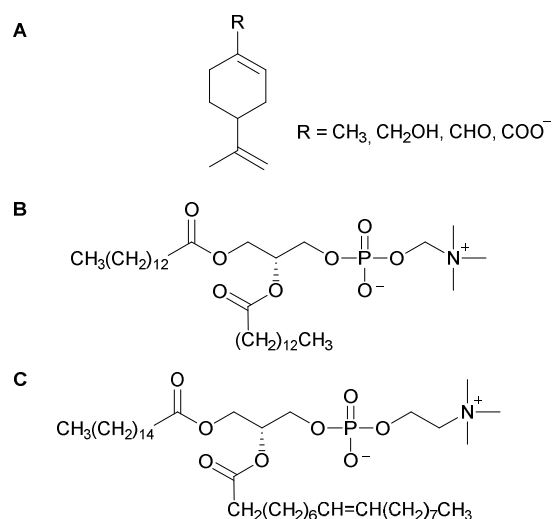
Fig. 18 Stuctures of terpenoids (A) evaluated by ITC for their interaction with model lipid bilayers of 1,2-dimyristoyl-*sn*-glycero-3-phosphocholine (DMPC, B) and 2-oleoyl-1-palmitoyl-*sn*-glycero-3-phosphocholine (POPC, C). **A**, limonene (R=CH₃), perillyl alcohol (R=CH₂OH), perillaldehyde (R=CHO) and deprotonated perillic acid (R=COO⁻); **B**, DMPC; **C**, POPC.

Fig. 19 Compounds evaluated by ITC for their interaction with lipids. **A**, cholesterol (β-OH), epicholesterol (α-OH); **B**, laurocapram; **C**, farnesol; **D**, ceramide 3; **E**, behenic acid.

able to form hydrogen bonds. Three of the tested terpenes (limonene, perillyl alcohol, and perillaldehyde) induced an extra order in the membrane and increase bilayer thickness, acting as "molecular glues" in a similar manner to cholesterol and epicholesterol (Fig. 19A). In contrary, the effect of deprotonated peryllic acid is based on alteration of lipid headgroup orientation. This behaviour can potentially influence the function of membrane-associated proteins and or even induce cell lysis, which could be responsible for its antimicrobial activity, although deeper investigation is necessary for confirmation.[99]

To investigate the implication of terpenes in transdermal drug delivery, Kang *et al.*[100,101] studied the interaction of laurocapram and farnesol (Fig. 19B and C), two skin penetration enhancers, with representative intercellular lipids of human stratum corneum. The ITC experiments were carried out using propylene glycol as solvent and indicated an enthalpy-driven binding (ΔH −229 kJ mol⁻¹) of laurocapram to ceramide-3 (Fig. 19D) with a 2:1 stoichiometry, whereas 1:1 interaction of laurocapram and cholesterol was mainly entropy driven. With behenic acid (Fig. 19E) no interaction was observed. Thus, laurocapram showed to be an effective enhancer which extracts cholesterol and binds ceramides without affecting the free fatty acid behenic acid.[100] A later study on the interaction between terpene farnesol and lipids cholesterol, behenic acid, ceramide 3, and ceramide-9[101] indicated binding rations of one for cholesterol and two for the other lipids. Interaction with behenic acid was exothermic and enthalpy driven, while the other binding thermodynamics were endothermic and entropy driven. Hydrogen bonding was supposed to be the main driving force.[101]
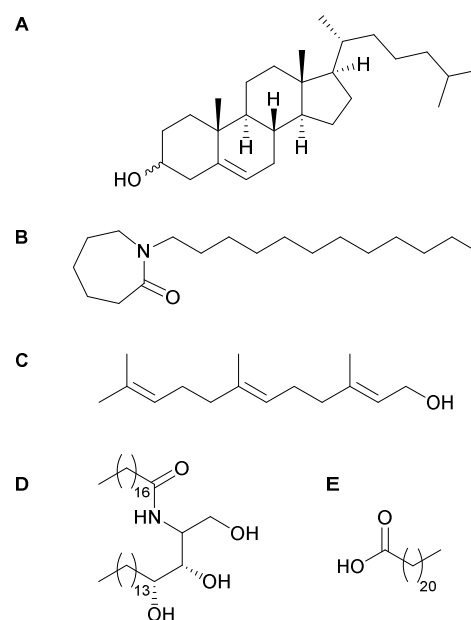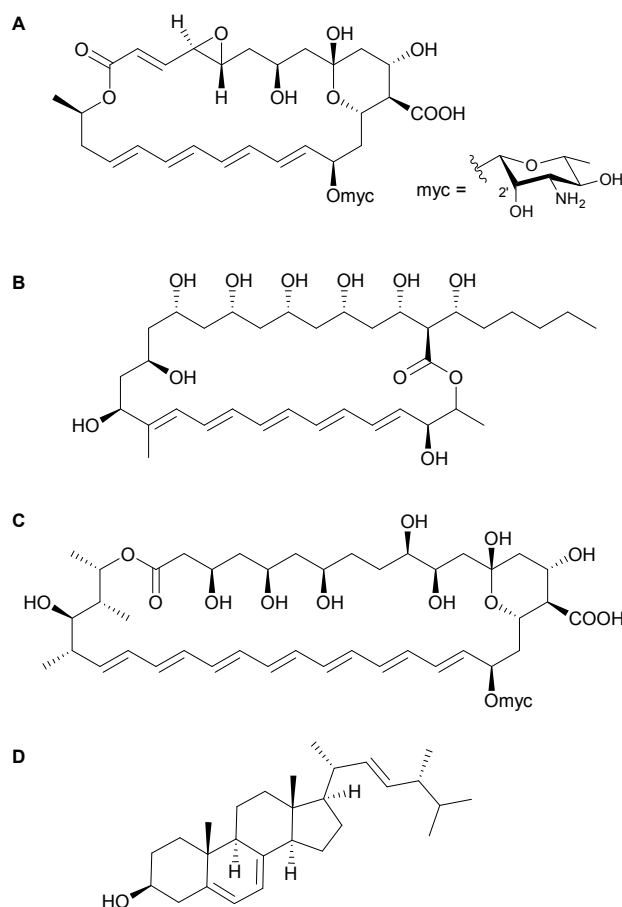

Fig. 20 Structures of polyene macrolides (A–C) evaluated for sterol (D) binding by ITC. **A**, natamycin; **B**, filipin; **C**, nystatin; **D**, ergosterol.

Interaction with Sterols. The polyene macrolide natamycin (Fig. 20A) is a commonly used antifungal agent in the clinic and food industry with a broad spectrum of activity without inducing resistance. To investigate the responsible mode of action, Welscher et al.[102] used ITC in combination with other techniques to study the interaction of this macrolide with phosphatidylcholine model membranes of varying sterol composition. The results were compared to those obtained for the polyene macrolides filipin and nystatin (Fig. 20B and C), which are known to cause leakage of essential components and cell death upon interaction with sterols. The ITC results showed no interaction of natamycin with the vesicles without sterols, whereas vesicles containing 10% of ergosterol (Fig. 20D) showed a significant amount of interaction. The binding constant of natamycin and ergosterol was estimated to be 5.7 × 10^4 M^{-1}, with a 1:1 or 1:2 stoichiometry, depending upon whether the sterol was available in the outer leaflet or in both leaflets of the membrane. Filipin binding did not seem to be dependent on sterol structure or the presence of sterols in the membrane. Nystatin binding to ergosterol (2.72 × 10^4 M^{-1}) was

similar to that of natamycin, and the latter was supposed to act via a novel mode of action blocking fungal growth by specific ergosterol binding. However, as the interaction resulted to be complex and no clear saturation could be observed, a more quantitative discussion on the binding data was not possible.[102]

In a similar manner, ergosterol binding is responsible of the antimycotic activity of the polyene macrolide amphotericin B (AmB, Fig. 21A). Unfortunately, AmB is highly toxic in human cells, limiting its clinical application as the last line of defence against systemic, often mortal, fungal infections. As cholesterol (Fig. 19A) binding is taken into account for the toxicity of this macrolide, several studies[103–106] with AmB and derivatives (Fig. 21A) were carried out to obtain an enhanced understanding of the involved sterol binding mechanism. In the study of Palacios et al.[103,104] a similar approach as reported for natamycin[102] was used, titrating a solution of AmB and derivatives with large unilamellar vesicles (LUV) of egg phophatidylcholine or 2-oleoyl-1-palmitoyl-sn-glycero-3-phosphocholine (POPC, Fig. 18C) containing 10% ergosterol (Fig. 20D), lanosterol (Fig. 21C), or without sterol. The results indicated a direct binding of AmB to membrane embedded sterol. Deletion of the mycosamine moiety (myc, Fig. 21A) abolished the sterol binding capacity (total exotherm with ergosterol of −39.75 and −25.94 μJ, respectively in AmdeB and MeAmdeB, vs. −159.00 and −284.93 μJ for AmB and MeAmB; similar values were obtained for AmB- and AmdeB–cholesterol interaction) and resulted in compounds without antifungal activity. These findings led to the conclusion that natamycin and amphotericin B exert their antifungal effects via mycosamine-mediated sterol binding and sterol sequestering. However, AmB, in addition, results in membrane permeabilization.[103] When the titrations were repeated with a C35 deoxygenated AmB derivative, total exotherms were similar to AmB. The ergosterol binding activity of this analogue was retained, but, in contrast to AmB, it was not able to permeabilize membranes.[104]
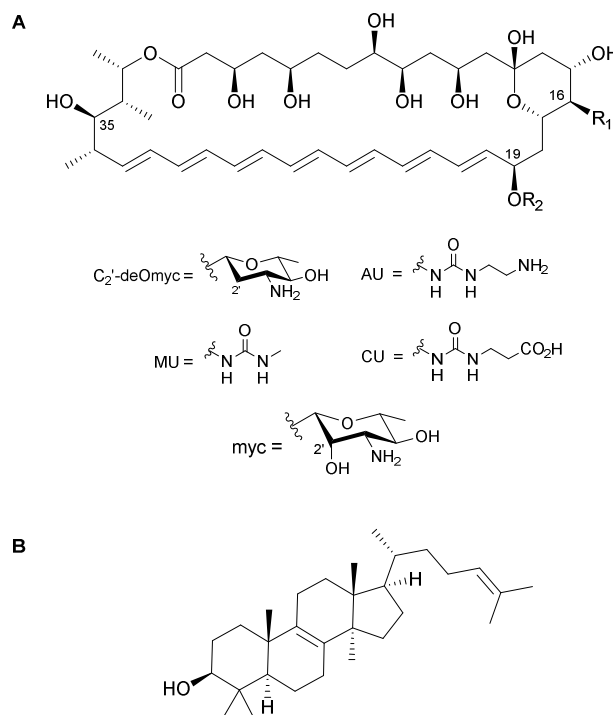
Fig. 21 Compounds evaluated to investigate the importance of functionalization in polyene macrolides in sterol binding by ITC. A, amphotericin B (AmB, R_1=CO_2H, R_2=myc) and derivatives MeAmB (R_1=CH_3, R_2=myc), AmdeB (R_1=CO_2H, R_2=OH), MeAmdeB (R_1=CH_3, R_2=OH), C2'-deOAmB (R_1=CH_3, R_2=C2'-deOmyc), AmBMU (R_1=MU, R_2=myc), AmBAU (R_1=AU, R_2=myc), and AmBCU (R_1=CU, R_2=myc); **C**, lanosterol.

In an ongoing study using the same methodology, the importance of the C2'-hydroxy group of the mycosamine moiety for the activity was evaluated by Wilcock et al.[105] AmB and two analogues, AmdeB and C-2'-deoxyamphotericin B (C2'-deAmB) (Fig. 21A), were studied for their ergosterol and cholesterol binding. The ITC data indicated that C2'-deOAmB showed a significant increase in ergosterol binding when compared to AmdeB, whereas no binding was observed with cholesterol. The selectivity was explained by a conformational change caused by the deletion of the C2'-hydroxy group, which resulted in different binding activities towards ergosterol and cholesterol. More importantly, the selectivity for ergosterol binding of AmbdeB and, in particular, C2'-deOAmB, showed no toxicity in in vivo assays, in contrast to highly toxic AmB. The observations made on the sterol binding mechanism of these macrolides were in strong contrast to leading models and showed that polar interactions between mycosamine and carboxylic groups on neighbouring AmB are not required for ion channel formation. Another result was that the C2'-hydroxy group of the mycosamine unit was not required for ergosterol binding. On the basis of these results, C2'-deOAmB was able to enter clinical studies.[105]

To deepen the knowledt in the field of AmB interactions, Davis et al.[106] focused on amphotericin B C16-urea analogues to obtain nontoxic, fungicidal AmB derivatives which, similar to C2'-deOAmB, did not bind cholesterol, which were

synthetically more accessible. Thus, they prepared AmB methyl urea (AmBMU), AmB amino urea (AmBAU), and Amb carboxylatoethyl urea (AmBCU) (Fig. 21A). The different assays showed that these compounds were acting as a sterol sponge that extracted the majority of ergosterol form the membranes of *Saccharomyces cerevisiae* and, thus, resulted in fungicidal activity. However, data obtained by ITC showed no binding to cholesterol (Fig. 19A), as this should result in decreased toxicity in humans. Thus, the combination of the ITC results with *in vitro* and *in vivo* studies suggested that AmBMU and AmBAU are promising candidates to replace AmB as less toxic agents in the treatment of invasive fungal infections and, furthermore, evade drug resistance. Additionally, the results supported a new ligand-selective allosteric-effect predicting that disruption of intramolecular polar interactions between functional groups on the macrolide core and the mycosamine moiety cause a conformational shift in the molecule. These observations result in a conformational change from a macrolide that binds both ergosterol and cholesterol to one that selectively binds ergosterol. This model could act as a guide for the rational development of other nontoxic amphotericins.

Interaction with Ions. Complexation with metal ions is necessary for a variety of biological activities. In this context, Liaw *et al.*[107] investigated Ca^{2+} binding of two natural acetogenins, annonacin and uvariamicin-I (Fig. 22A and B), by ITC and NMR experiments, and the implication of calcium ion chelating ability in their cytotoxic activity. ITC data indicated that both acetogenins interacted with Ca^{2+} in an exothermic sequential binding process, concluding that their chelating ability with calcium ions is one of the key factors in the compound's cytotoxic activity.
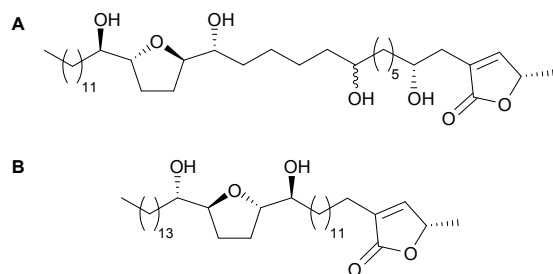

Fig. 22 Compounds evaluated by ITC for their Ca^{2+} binding. A, annonacin; **B**, uvariamicin-I.

***In vivo* Interactions of Natural Products**. As pointed out in the previous sections, isothermal titration calorimetry (ITC) is a powerful, well-established method to analyse molecule–natural product interactions in non-living systems. However, to study physiologically relevant interactions, stoichiometry, and binding kinetics are necessary to be evaluated in a living organism, which cannot be addressed by techniques, such as NMR, X-ray diffraction, or surface plasmon resonance. The advantages of thermodynamic assays in a living system are obvious, as low solubilities, purification, and crystallization problems are limiting the analysis by NMR spectroscopy or X-ray diffraction, which is of particular interest for the study of

membrane-bound proteins. On the other hand, fluorescent spectroscopy, photoaffinity labelling, and homology modelling provide only indirect biophysical information on the interaction. Thus, the application of ITC in living cell systems would be beneficial to study the net interaction between receptor and ligand, although their thermal dynamics are complex and poorly understood. An additional problem for ITC experiments with living cells is that they exert intrinsic metabolic heat although they are in unstimulated standard culture conditions. Therefore, the subtraction of thermal events that are not specifically caused by receptor-ligand complexation is necessary for evaluation by ITC.

In this context, Hirakura *et al*. and Ikeda *et al*.[108,109] reported the application of ITC in living cells to study the interaction between metabotropic glutamate receptor-1α (mGluR1), a transmembrane protein of the family of G-protein-coupled receptors, and the agonist (*S*)-3,5-dihydroxyphenylglycine (DHPG, Fig. 23A). In a first approach, CHO cells overexpressing mGluR1 (CHO-mGluR1α) and wild type CHO-k1 cells were titrated with the ligand DHPG to evaluate the molecular mechanisms underlying the inhibitory effects of D_2O on the IP_3-mediated Ca^{2+} signalling pathway. After subtraction

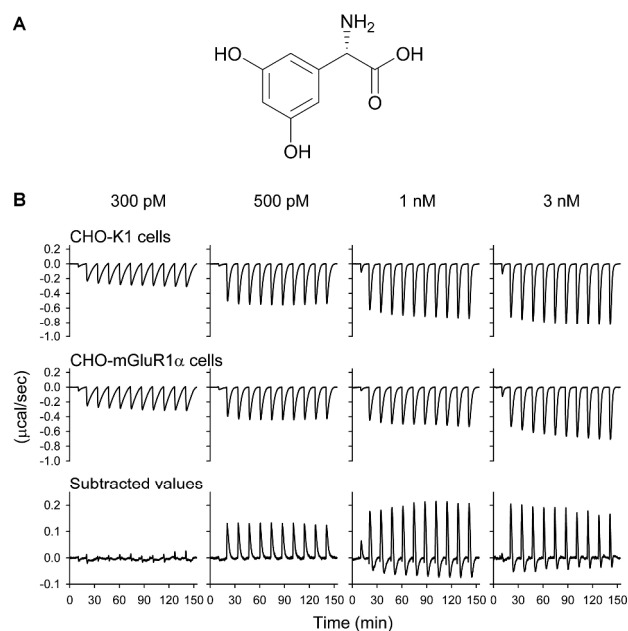**Fig. 23 Application of ITC in living cells to study the interaction between metabotropic glutamate receptor-1α and the agonist (*S*)-3,5-dihydroxyphenylglycine (DHPG). A**, Structure of DHPG; **B**, Concentration-dependent thermal responses via repeated titration of DHPG. DHPG concentrations in the injection syringe are shown at the top. All recordings were conducted at 20°C. Subtracted traces demonstrated that the critical concentration which activates receptor-dependent thermal responses is located between 300–500 pM. Titration with 500 pM DHPG generated heat absorption (as + µcal/s) but not heat production (as − µcal/s). The size of heat absorption and production is maximized at 1 nM and then gradually reduced at 3 nM.[109] Reprinted from: Protocol Exchange, doi:10.1038/ protex.2013.061, Ikeda, M.; Takeda, M.; Yoshioka, T. Thermal dynamics of metabotropic glutamate receptor signaling revealed by subtraction micro-calorimetric measurements on live cells. Copyright (2013), public Creative Commons Attribution-NonCommercial licence (http://creativecommons.org/licenses/by-nc/3.0/).

of thermal responses from these cells, the thermograms showed biphasic thermal events upon DHPG–mGluR1 interaction. That way, application of agonist DHPG to cell suspensions in H_2O medium generated a heat peak of 470 μJ at 200 s, which was attributed to the activation of mGluR1 in CHO cells. In wild-type CHO cells, which do not express mGluR1, no heat generation was observed, indicating that the Ca^{2+} level did not change. The repetition of the ITC experiment in 90% D_2O medium showed a greater initial differential calorimetric change, and the total amount of heat was reduced to 146 μJ. The overall results suggested that DHPG application induced a conformational change in G-protein-coupled receptors and/or trimeric G proteins, which were responsible for the changes in heat production and absorption. Furthermore, the replacement of hydrogen with deuterium was suggested to induce a reduction in hydrogen bond frequency, leading to a modification of bio-signalling and bio-energetic processes.[108]

In the more recent approach of Ikeda *et al*.[109], a minimization of the differential power, which compensates the temperature difference between recording- and reference chamber in the ITC equipment, should enhance the sensitivity of the measurements. Initial stabilization difficulties due to cell death and/or metabolic activities during the recordings over 4–5 hours at 30 ºC were resolved by using protease inhibitor cocktails in reduced $CaCl_2$ buffer and temperature reduction to 20 ºC (Fig. 23B). That way, it was possible to characterize mGluR1–DHPG interactions and to estimate the thermal dynamics underlying receptor-to-ligand interactions including heats and entropy change (ΔH −0.08 kJ mol^{-1}, $-T\Delta S$ −58.8 kJ mol^{-1} at 293 K), dissociation constant (K_d 33.33 pM), and the number of binding sites (47000 per living cell). These data can help to elucidate the downstream intracellular signalling linked to receptor activation.[109]

Conclusions

Isothermal titration calorimetry (ITC) is a well-established technique in the drug design practise because it provides accurate characterization of binding thermodynamics, with no requirement for chemical modification or labelling. This information would be difficult to achieve with other methods. Nevertheless, the main goal for ITC users is to develop accurate structure/energy functions to predict the relationships between structural parameters and the enthalpic and entropic forces driving molecular interactions. This would be of paramount importance for understanding biomolecular interactions as well as assisting the optimization of ligand binding affinities. Although ITC has demonstrated to be a reliable tool for the analysis of biomolecular interactions and the best way to dissect the thermodynamic components there are still some concerns about the interpretation of such data in particular regarding the enthalpy-entropy compensation phenomenon. Nevertheless, ITC has been able to shed light on unknown interactions, to revise some well-established leading models, and to give rise to compounds that reached clinical studies.

It is thus not surprising that this technique is increasingly used to characterize the manifold interactions of natural products, as they are able to interact powerfully with a huge number of different molecules, including proteins, nucleic acids, macrocyclic oligosaccharides and other types of molecules. The broad scope of this technique makes it a powerful tool for the identification of biomolecular targets for natural products, when used in combination with liquid chromatography.[14] Additionally, modern ITC instrumentation with high sensitivity (μg of sample) and automation mechanisms together with the absence of specific structural prerequisites (cromophores, etc.) allows the use of this technique in secondary screening programs of low molecular weight compounds.[30]

Current trends in drug design suggest that compounds with favourable enthalpy terms are likely to make the best lead compounds. This has been rationalized in terms of better complementarity, as enthalpic terms are associated with specific interactions (bond formation). Along those lines, analysis of a calorimetry database (SCORPIO) reveals that protein-natural products interactions are generally characterized for being less entropically driven than those for synthetic compounds.[12] This is probably a consequence of the current protocols applied in ligand optimization, as the easiest way to improve binding affinities is to attach atoms that get buried upon binding, increasing the entropic term of the interaction. The previous observation about the nature of the thermodynamic forces driving natural products interactions, is somehow predictable as they are privileged structures specifically designed by nature, but reinforces the important role of natural products in drug discovery.

Even more, the extension of the application of this technique on living organisms is only a starting point to convert ITC into a powerful tool in the future for the evaluation of biochemical pathways, the mechanisms of actions involved in compound's bioactivity, or its evaluation for technical applications.

Notes and references

[a] Institute of Bioorganic Chemistry "Antonio González", Center for Biomedical Research of the Canary Islands, University of La Laguna, Avenida Astrofísico Francisco Sánchez 2, 38206 La Laguna, Santa Cruz de Tenerife, Spain.

1   M. Kabiri, L. D. Unsworth, *Biomacromol*., 2014, **15**, 3463.

2   R. Ghai, R. J. Falconer, B. M. Collins, *J. Mol. Recognit*., 2012, **25**, 32.

3   D. Burnouf, E. Ennifar, S. Guedich, B. Puffer, G. Hoffmann, G. Bec, F. Disdier, M. Baltzinger, P. Dumas, *J. Am. Chem. Soc*., 2011, **134**, 559.

4   J. E. Ladbury, G. Klebe, E. Freire, *Nat. Rev. Drug Discov.*, 2010, **9**, 23.

5   K. Rajarathnam, J. Rösgen, *Biochim. Biophys. Acta*, 2014, **1838**, 69.

6   E. Freire, *Drug Discov. Today*, 2004, **1**, 295.

7   Y.-L. Zhang, Z.-Y. Zhang, *Anal. Biochem.*, 1998, **261**, 139.

8   B. Sigurskjold, *Anal. Biochem.*, 2000, **277**, 260.

9   W. B. Turnbull, A. H. Daranas, *J. Am. Chem. Soc.*, 2003, **125**, 14859.

10 J. E. Ladbury, B. Z. Chowdhry, *Chem. Biol.*, 1996, **3**, 791.

11 A. Schön, A. Velázquez-Campoy, *Methods for Structural Analysis of Protein Pharmaceuticals*, ed. W. Jiskoot, D. J. A. Crommelin, AAPS Press, Arlington VA, 2005, 573.

12 T. S. G. Olsson, M. A. Williams, W. R. Pitt, J. E. Ladbury, *J. Mol. Biol.*, 2008, **384**, 1002.

13 L. S. Roselin, M.-S. Lin, P.-H. Lin, Y. Chang, W.-Y. Chen, *Biotechnol. J.*, 2010, **5**, 85.

14 X. Zhou, R. M. Kini, J. Sivaraman, *Nat. Protoc.*, 2011, **6**, 158.

15 J.-P. E. Grolier, J. M. del Río, *J. Chem. Thermodyn.*, 2012, **55**, 193.]

16 J. D. Chodera, D. L. Mobley, *Annu. Rev. Biophys.*, 2013, **42**, 121.

17 M. Neeb, P. Czodrowski, A. Heine, L. J. Barandun, C. Hohn, F. Diederich, G. Klebe, *J. Med. Chem.*, 2014, **57**, 5554.

18 A. Brown, *Int. J. Mol. Sci.*, 2009, **10**, 3457.

19 T. Wiseman, S. Williston, J. F. Brandts, L.-N. Lin, *Anal. Biochem.*, 1989, **179**, 131.

20 I. Herrera, M. A. Winnik, *J. Phys. Chem. B*, 2013, **117**, 8659.

21 P. Atkins, J. de Paula, *Physical Chemistry,* Oxford University Press, *9th Edition*, 2010.

22 J. D. Chodera, D. L. Mobley, *Annu. Rev. Biophys.,* 2013, **42**, 121.

23 M. C. Chervenak, E. J. Toone, *J. Am. Chem. Soc.,* 1994, **116**, 10533.

24 C. A. MacRaild, A. Hernández Daranas, A. Bronowska, S. W. Homans. *J. Mol. Biol.*, 2007, **368**, 822.

25 J. Tellinghuisen, J. D. Chodera, *Anal. Biochem.*, 2011, **414**, 297.

26 R. N. Goldberg, N. Kishore, R. M. Lennen, J. Phys. Chem. Ref. Data, 2002, **31**, 231.

27 B. M. Baker, K. P. Murphy, *Biophys. J.*, 1996, **71**, 2049.

28 V. Karlsen, E. B. Heggset, M. Sørlie, *Thermochim. Acta*, 2010, **501**, 119.

29 M. J. Limo, C. C. Perry, A. A. Thyparambil, Y. Wei, R. A. Latour, *Bio-Inspired Nanotechnology*, ed. M. R. Knecht, T. R. Walsh, Springer, New York, 2014, 37.

30 E. H. Mashalidis, P. Śledź, S. Lang, C. Abell, *Nat. Protoc.*, 2013, **8**, 2309.

31 S. Arioli, E. Ragg, L. Scaglioni, D. Fessas, M. Signorelli, M. Karp, D. Daffonchio, I. De Noni, L. Mulas, M. Oggioni, S. Guglielmetti, D. Mora, *PLoS ONE*, 2010, **5**, e15520, doi:10.1371/journal.pone.0015520.

32 J. E. Ladbury, *Biotechniques*, 2004, **37**, 885.

33 T. L. Nero, C. J. Morton, J. K. Holien, J. Wielens, M. W. Parker, *Nat. Rev. Cancer*, 2014, **14**, 249.

34 C. Poncet-Legrand, C. Gautier, V. Cheynier, A. Imberty, *J. Agric. Food Chem.*, 2007, **55**, 9235.

35 J. M. McRae, R. J. Falconer, J. A. Kennedy, *J. Agric. Food Chem.*, 2010, **58**, 12510.

36 S. Pal, S. K. Dey, C. Saha, PLoS One, 2014, 9, e102460.

37 Y.-T. Tung, C.-A. Hsu, C.-S. Chen, S.-C. Yang, C.-C. Huang, S.-T. Chang, *J. Agric. Food Chem.*, 2010, **58**, 9936.

38 G. Budryn, B. Pałecz, D. Rachwał-Rosiak, J. Oracz, D. Zaczyńska, S. Belica, I. Navarro-González, J. M. V. Meseguer, H. Pérez-Sánchez, *Food Chem.*, 2015, **168**, 276.

39 H. Zhang, R. Zhou, L. Li, J. Chen, L. Chen, C. Li, H. Ding, L. Yu, L. Hu, H. Jiang, X. Shen, *J. Biol. Chem.*, 2011, **286**, 1868.

40 R. A. Fazier, A. Papadopoulou, I. Mueller-Harvey, D. Kissoon, R. J. Green, *J. Gric. Food Chem.*, 2003, **51**, 5189.

41 R. A. Frazier, A. Papadopoulou, R. J. Green, *J. Pharm. Biomed. Anal.*, 2006, **41**, 1602.

42 S. Pal, C. Saha, M. Hossain, S. K. Dey, G. S. Kumar, *PLoS ONE*, 2012, **7**, e43321, doi:10.1371/journal.pone.0043321.

43 J. Xi, L. Fan, *J. Therm. Anal. Calorim.*, 2010, **102**, 217.

44 S.-H. Wang, F.-F. Liu, X.-Y. Dong, Y. Sun, *J. Phys. Chem. B*, 2010, **114**, 11576.

45 S.-H. Wang, X.-Y. Dong, Y. Sun, *J. Phys. Chem. B*, 2012, **116**, 5803.

46 D. B. B. Trivella, L. Bleicher, L. d. C. Palmieri, H. J. Wiggers, C. A. Montanari, J. W. Kelly, L. M. T. R. Lima, D. Foguel, I. Polikarpov, *J. Struct. Biol.*, 2010, **170**, 522.

47 N. S. Green, T. R. Foss, J. W. Kelly, *Proc. Natl. Acad. Sci. U.S.A.*, 2005, **102**, 14545.

48 C. Daniels, A. Daddaoua, D. Lu, X. Zhang, J.-L. Ramos, *J. Biol. Chem*, 2010, **285**, 21372.

49 W. Arif, S. Xu, D. Isailovic, W. J. Geldenhuys, R. T. Carroll, M. O. Funk Jr., *Biochemistry*, 2011, **50**, 5806.

50 Z. Yukel, E. Avci, Y. K. Erdem, *Food Chem.*, 2010, **121**, 450.

51 P. F. Egea, A. Mitschler, N. Rochel, M. Ruff, P. Chambon, D. Moras, *EMBO J.*, 2000, **19**, 2592.

52 P. F. Egea, A. Mitschler, D. Moras, *Mol. Endocrinol.*, 2002, **16**, 987.

53 V. Nahoum, E. Pérez, P. Germain, F. Rodríguez-Barrios, F. Manzo, S. Kammerer, G. Lemaire, O. Hirsch, C. A. Royer, H. Gronemeyer, A. R. de Lera, W. Bourguet, *Proc. Natl. Acad. Sci. U.S.A.*, 2007, **104**, 17323.

54 A. P. Brogan, W. R. Widger, D. Bensadek, I. Riba-Garcia, S. J. Gaskell, H. Kohn, *J. Am. Chem. Soc.*, 2005, **127**, 2741.

55 N. Keswani. S. Choudhary, N. Kishore, *J. Biochem.*, 2010, **148**, 71.

56 A. A. Thoppil, R. Sharma, N. Kishore, *Biopolymers*, 2008, **89**, 831.

57 J. Fanghänel, G. Fischer, *Biophys. Chem.*, 2003, **100**, 351.

58 P. R. Connelly, J. A. Thomson, M. J. Fitzgibbon, F. J. Bruzzese, *Biochemistry*, 1993, **32**, 5583.

59 A. Cipres, D. P. O'Malley, K. Li, D. Finlay, P. S. Baran, K. Vuori, *ACS Chem. Biol.*, 2010, **5**, 195.

60 M. Hossain, A. Y. Khan, G. S. Kumar, *PLoS ONE*, 2011, **6**, e18333, doi:10.1371/journal.pone.0018333.

61 S. Hazra, M. Hossain, G. S. Kumar, *Mol. BioSyst.*, 2013, **9**, 143.

62 M. N. Zakharov, S. Bhasin, T. G. Travison, R. Xue, J. Ulloor, R. S. Vasan, E. Carter, F. Wu, R. Jasuja, *Mol. Cell. Endocrinol.*, 2015, **399**, 190.

63 E. Kachooei, A. A. Moosavi-Movahedi, F. Khodagholi, F. Mozaffarian, P. Sadeghi, H. Hadi-Alijandvand, A. Ghasemi, A. A. Saboury, M. Farhadi, N. Sheibani, *J. Biochem.*, 2014, **155**, 361.

64 P. Domadia, S. Swarup, A. Bhunia, J. Sivaraman, D. Dasgupta, *Biochem. Pharmacol.*, 2007, **74**, 831.

65 X. Li, G. Wang, D. Chen, Y. Lu, *Mol. BioSyst.*, 2014, **10**, 326.

66 L. Aberkane, J. Jasniewski, C. Gaiani, J. Scher, C. Sanchez, *Langmuir*, 2010, **26**, 12523.

67 T. Vinayahan, P. A. Williams, G. O. Phillips, *Biomacromol.*, 2010, **11**, 3367.

68 K. Bhadra, M. Maiti, G. S. Kumar, *Biochim. Biophys. Acta*, 2008, **1780**, 1054.

69 M. M. Islam, S. R. Chowdhury, G. S. Kumar, *J. Phys. Chem. B*, 2009, **113**, 1210.

70 M. M. Islam, R. Sinha, G. S. Kumar, *Biophys. Chem.*, 2007, **125**, 508.

71 M. M. Islam, P. Pandya, S. R. Chowdhury, S. Kumar, G. S. Kumar, *J. Mol. Struct.*, 2008, **891**, 498.

72 K. Bhadra, M. Maiti, G. S. Kumar, *Biochim. Biophys. Acta*, 2007, **1770**, 1071.

73 K. Bhara, M. Maiti, G. S. Kumar, *Chem. Biodivers.*, 2008, **5**, 575.

74 K. Bhadra, G. S. Kumar, *Med. Res. Rev.*, 2011, **6**, 821.

75 A. Adhikari, M. Hossain, M. Maiti, G. S. Kumar, *J. Mol. Struct.*, 2008, **889**, 54.

76 M. Hossain, G. S. Kumar, *J. Chem. Thermodyn.*, 2009, **41**, 764.

77 M. Hossain, G. S. Kumar, *J. Chem. Thermodyn.*, 2010, **42**, 1273.

78 P. Giri, G. S. Kumar, *Biochim. Biophys. Acta*, 2007, **1770**, 1419.

79 M. Hossain, A. Kabir, G. S. Kumar, *J. Biomol. Struct. Dyn.*, 2012, **30**, 223.

80 P. Basu, D. Bhowmik, G. S. Kumar, *J. Photochem. Photobiol. B*, 2013, **129**, 57.

81 P. Basu, G. S. Kumar, *J. Photochem. Photobiol. B*, 2014, **138**, 282.

82 M. M. Islam, G. S. Kumar, *J. Mol. Struct.*, 2008, **875**, 382.

83 G. S. Kumar, *J. Biosci.*, 2012, **37**, 539.

84 A. Das, K. Bhadra, G. S. Kumar, *PLoS ONE*, 2011, **6**, e23186, doi:10.1371/journal.pone.0023186.

85 M. A. D. Neves, O. Reinstein, P. E. Johnson, *Biochemistry*, 2010, **49**, 8478.

86 M. A. D. Neves, O. Reinstein, M. Saad, P. E. Johnson, *Biophys. Chem.*, 2010, **153**, 9.

87 A. Basu, G. S. Kumar, *Int. J. Biol. Macromol.*, 2013, **62**, 257.

88 T. Zhang, Z. Wu, J. Du, Y. Hu, L. Liu, F. Yang, Q. Jin, *PLoS ONE*, 2012, **7**, e30259, doi:10.1371/journal.pone.0030259.

89 D. Ghosh, S. K. Dey, C. Saha, *PLoS ONE*, 2014, **9**, e84880, doi:10.1371/journal.pone.0084880.

90 D. Ghosh, C. Saha, M. Hossain, S. K. Dey, G. S. Kumar, *J. Biomol. Struct. Dyn.*, 2013, **31**, 331.

91 K. Bouchemal, S. Mazzaferro, *Drug Discov. Today*, 2012, **17**, 623.

92 M. R. de Jong, J. F. J. Engbersen, J. Huskens, D. N. Reinhoudt, *Chem. Eur. J.*, 2000, **6**, 4034.

93 Y. Chen, F. Li, B.-W. Liu, B.-P. Jiang, H.-Y. Zhang, L.-H. Wang, Y. Liu, *J. Phys. Chem. B*, 2010, **114**, 16147.

94 C. Danel, C. Duval, N. Azaroual, C. Vaccher, J.-P. Bonte, C. Bailly, D. Landy, J.-F. Goossens, *J. Chromatogr. A*, 2011, **1218**, 8708.

95 Y. Liu, G.-S. Chen, Y. Chen, D.-X. Cao, Z.-Q. Ge, Y.-J. Yuan, *Bioorg. Med. Chem.*, 2004, **12**, 5767.

96 S. Mazzaferro, K. Bouchemal, J.-F. Gallard, B. I. Iorga, M. Cheron, C. Gueutin, C. Steinmesse, G. Ponchel, *Int. J. Pharm.*, 2011, **416**, 171.

97 F. Segura-Sanchez, K. Bouchemal, G. Lebas, C. Vauthier, N. S. Santos-Magalhaes, G. Ponchel, *J. Mol. Recognit.*, 2009, **22**, 232.

98 D.-Z. Sun, L. Li, X.-M. Qiu, F. Liu, B.-L. Yin, *Int. J. Pharm.*, 2006, **316**, 7.

99 S. Witzke, L. Duelund, J. Kongsted, M. Petersen, O. G. Mouritsen, H. Khandelia, *J. Phys. Chem. B*, 2010, **114**, 15825.

100 L. Kang, P. C. Ho, S. Y. Chan, *J. Therm. Anal. Calorim.*, 2006, **1**, 27.

101 L. Kang, V. H. Kumar, P. F. C. Lim, H. H. Cheong, S. Y. Chan, *Natural Products*, ed. K. G. Ramawat, J. M. Mérillon, Springer, Berlin Heidelberg, 2013, 3757.

102 Y. M. te Welscher, H. H. ten Napel, M. M. Balagué, C. M. Souza, H. Riezman, B. de Kruijff, E. Breukink. *J. Biol. Chem.*, 2008, **283**, 6393.

103 D. S. Palacios, I. Dailey, D. M. Siebert, B. C. Wilcock, M. D. Burke, *Proc. Natl. Acad. Sci. U.S.A.*, 2011, **108**, 6733.

104 K. C. Gray, D. S. Palacios, I. Dailey, M. M. Endo, B. E. Uno, B. C. Wilcock, M. D. Burke, *Proc. Natl. Acad. Sci. U.S.A.*, 2012, **109**, 2234.

105 B. C. Wilcock, M. M. Endo, B. E. Uno, M. D. Burke, *J. Am. Chem. Soc.*, 2013, **135**, 8488.

106 S. A. Davis, B. M. Vincent, M. M. Endo, L. Whitesell, K. Marchillo, D. R. Andes, S. Lindquist, M. D. Burke, *Nat. Chem. Biol.*, 2015, **11**, 481.

107 C.-C. Liaw, Y.L. Yang, M. Chen, F.-R. Chang, S.-L. Chen, S.-H. Wu, Y.-C. Wu, *J. Nat. Prod.*, 2008, **71**, 764.

108 Y. Hirakura, T. Sugiyama, M. Takeda, M. Ikeda, T. Yoshioka, *Biochim. Biophys. Acta*, 2011, **1810**, 218.

109 M. Ikeda, M. Takeda, T. Yoshioka, *Protocol Exchange*, 2013, doi:10.1038/protex.2013.061.